synthesized protein. Activation of PERK phosphorylates the α subunit of eukaryotic initiation factor 2 (eIF2α), which inhibits protein synthesis and hence decreases the protein load on the ER. Phosphorylation of eIF2α is also induced by a variety of stress stimuli. Depending on the nature of the stress stimuli, eIF2α can be phosphorylated by four different eIF2α kinases: PKR which is stimulated by viral infection, general control non-derepressible-2 (GCN2) activated by amino acid starvation, PERK stimulated by disrupted ER homeostasis and heme-regulated inhibitor (HRI) activated by iron deficiency.[7] Global attenuation of protein biosynthesis then paradoxically increases expressions of several proteins including the transcription factor activating transcription factor-4 (ATF4).[8] This eIF2α phosphorylation-dependent, stress-inducible pathway has been referred to as the integrated stress response (ISR).[8,9]

We have recently shown that the *Eif4ebp1* gene, encoding eukaryotic initiation factor 4E (eIF4E)-binding protein 1 (4E-BP1), a translational suppressor, is a direct target of the transcription factor ATF4, and demonstrated that translational control mediated by 4E-BP1 induction plays an important role in maintaining β-cell homeostasis under ER stress conditions.[10] 4E-BP1 protein is present in three forms with different phosphorylation states. The non-phosphorylated α form is the most active in terms of eIF4E binding and the hyperphosphorylated γ form is inactive with the β form being intermediated. Thus, 4E-BP1 activity can be modulated by its phosphorylation and dephosphorylation. Since oxidative stress, which also activates the ISR, is another important contributor of β-cell loss during development of type 2 diabetes mellitus,[4,11] we examined expression of 4E-BP1 in mouse insulinoma MIN6 cells treated with arsenite, an inducer of oxidative stress.[12,13] We found that ISR induced by oxidative stress increased 4E-BP1 expression while the c-Jun N-terminal kinase (JNK) pathway activated by the stress condition suppressed it. Furthermore, oxidative stress caused dephosphorylation of 4E-BP1 and hence its activation in a JNK-dependent manner. These modulations of 4E-BP1 expression and phosphorylation may contribute to fine tuning of translational control under stress conditions.

MATERIALS AND METHODS

MIN6 cell culture cell viability assay

MIN6 cells were cultured in DMEM supplemented with 15% fetal calf serum (FCS) and 450 mg ml^{-1} glucose. Cells were seeded at 1 or 4×10^5 cells per well in 24-multiwell plates. Two days later, cells were treated with thapsigargin (0.5 μM) or arsenite (15 μM). Cell viability was determined with a cell proliferation assay kit (Promega).

Western blotting

Cell lysates were subjected to SDS-PAGE and probed with primary antibodies purchased from the following companies: anti-4E-BP1 (Cell Signaling), anti-ATF4 (Santa Cruz), anti-CHOP (Santa Cruz), anti-actin (Sigma), anti-phospho-eIF2α (Cell Signaling), anti-XBP1 (Santa Cruz), anti-KDEL (Stressgen), anti-phospho-JNK (Cell Signaling), anti-total-JNK (Cell Signaling), anti-total-c-Jun (Cell Signaling), anti-phospho-c-Jun (Cell Signaling), anti-total-S6 ribosomal protein (Cell Signaling), and anti-phospho-S6 ribosomal protein (Cell Signaling). Western blot experiments were performed at least three times.

Quantitative real-time RT-PCR

Total ribonucleic acid (RNA) was extracted from MIN6 cells using ISOGEN (Nippon Gene). For real-time reverse transcription polymerase chain reaction (RT-PCR) analysis, complementary DNA was synthesized by reverse transcription (RT) using the oligo $d(T)_{16}$ primer and subjected to polymerase chain reaction (PCR) amplification with gene-specific primers using a SYBR Green 1 kit (Roche). Data are presented as relative values to GAPDH mRNA. The specific primers for 4E-BP1 were 5′-GGGGACTACAGCACCACTCC-3′ and 5′-ATCGCTGGTAGGGGCTAGTGA-3′.

Statistical analysis

Data are presented as means ± SEM. Differences between groups were assessed by Student's t test. $p < 0.05$ was considered significant.

RESULTS

We examined expression of ATF4, master regulator of stress signaling pathways governing the ISR, in MIN6 cells treated with thapsigargin and arsenite. We used 0.5 μM thapsigargin for induction of ER stress and 15 μM arsenite for oxidative stress, since these concentrations of agents induced ATF4 over the range of time course, although cell death was evident after 16 h in MIN6 cells treated with arsenite. Time course of ATF4 induction was different between thapsigargin and arsenite: arsenite induced expression of ATF4 more rapidly (Figure 1A). ATF4 expression was highest at 8 h for thapsigargin and 6 h for arsenite after initiation of the drug exposure. ATF4 expression clearly declined at 24 h, for thapsigargin, and 12 h, arsenite, after treatment with these agents. Thus, we examined effects of these agents at 0, 8 and 24 h for thapsigargin and 0, 6, and 12 h for arsenite in the following experiments.

Phosphorylation of eIF2α, the initial event in the ISR signaling, was comparable between MIN6 cells treated with thapsigargin and arsenite (Figure 1B). As expected, C/EBP-homologous protien (CHOP), one of the transcriptional targets of ATF4 was similarly induced with thapsigargin and arsenite in MIN6 cells, at time points when two agents caused similar induction of ATF4. However, expression of 4E-BP1 protein, another target of ATF4, was much less in MIN6 cells treated with arsenite (Figure 1B). We also used 30 or 60 μM arsenite and found that 4E-BP1 induction was not increased or even diminished (data not shown). We also

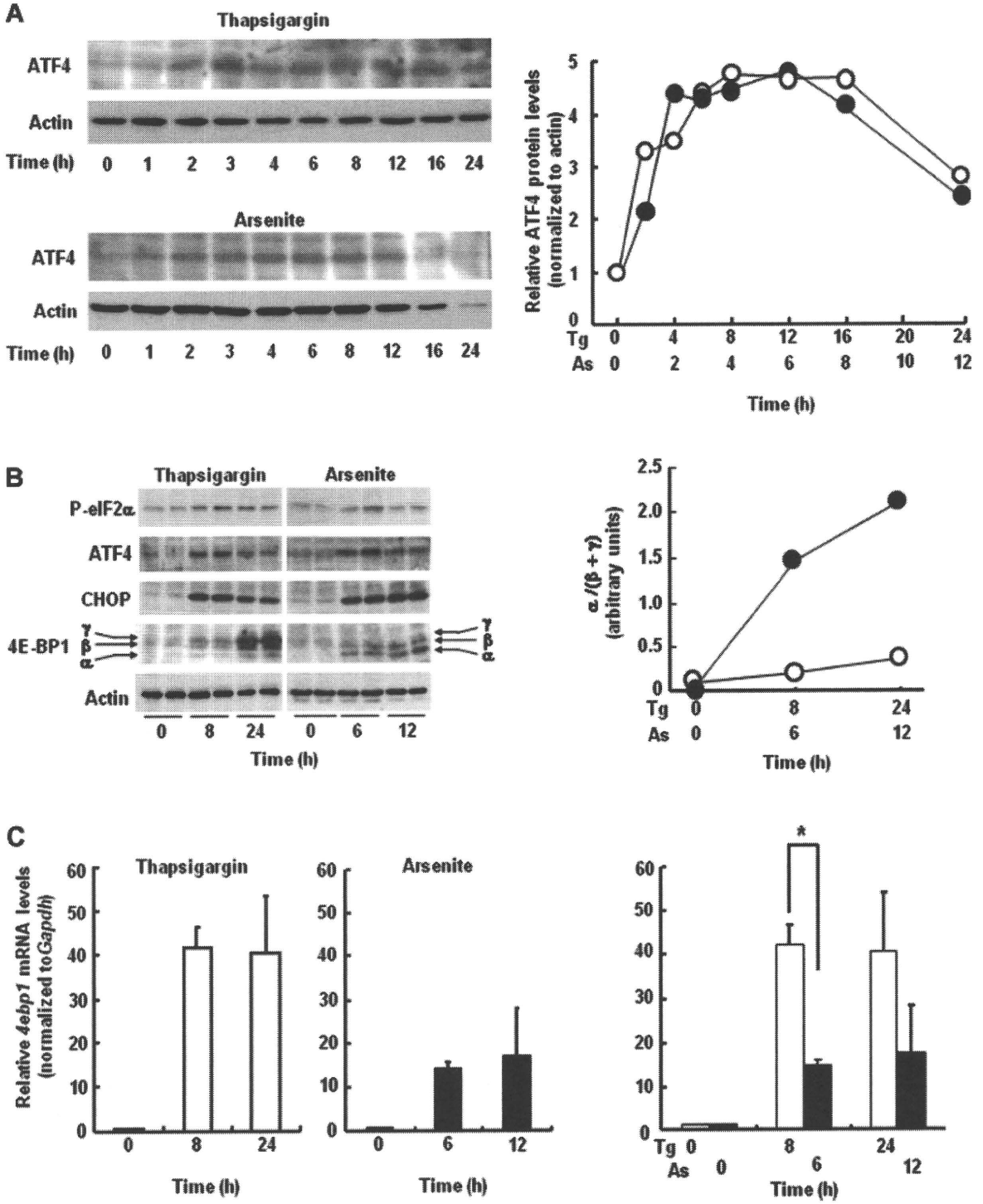

Figure 1. Time courses of ATF4 expression and responses of eIF2α/ATF4 pathway in MIN6 cells under ER stress or oxidative stress conditions. (A) Time courses of ATF4 expression were examined in MIN6 cells treated with 0.5 μM thapsigargin or 15 μM arsenite for indicated time periods. The ratio of ATF4/actin protein levels in MIN6 cells treated with thapsigargin (open circles) or arsenite (closed circles) is also presented graphically after quantification using the Image-J program. (B) MIN6 cells were treated with thapsigargin (0.5 μM) or arsenite (15 μM) for indicated time periods, subjected to SDS-PAGE and probed with the indicated antibodies: P-eIF2α, phosphorylated-eIF2α. Western blot data shown are representative of at least three experiments with different sets of samples. The intensities of three forms of 4E-BP1 bands induced by thapsigargin (open circles) or arsenite (closed circles) were quantified and the ratio of the α form to the sum of β and γ forms are shown in the right. Thapsigargin, (open circles) or arsenite (closed circles). (C) Total RNA was isolated from MIN6 cells treated with thapsigargin (0.5 μM) or with arsenite (15 μM). Relative mRNA levels of *4ebp1* transcript were obtained after normalization to *Gapdh* mRNA levels. Data from three experiments are summarized. To make comparison easier, relative *4ebp1* mRNA levels induced by thapsigargin (open bars) or arsenite (closed bars) was shown in a single panel (right panel) and statistically analyzed. $n = 3$, $^{*}p < 0.05$

found that phosphorylation status of 4E-BP1 was different between MIN6 cells treated with thapsigargin and arsenite: arsenite increased non-phosphorylated α form of the translational suppressor, while ER stress inducer increased 4E-BP1 protein levels with basically no changes in its phosphorylation status (Figure 1B). Quantitative RT-PCR analysis showed that the arsenite-induced 4E-BP1 transcript level was one-third of that induced thapsigargin in MIN6 cells (Figure 1C).

In order to get insight into different induction of 4E-BP1 between ER stress and oxidative stress, we compared expressions of several proteins involved in the UPR or the oxidative stress signaling pathway. Expression of glucose-regulated protein 78 Da (GRP78; Figure 2A), a target of the ATF6 pathway, and that of XBP-1 (Figure 2B), involved in the IRE-1 pathway of the UPR, were induced by thapsigargin but not arsenite. JNK activation was reported in response to ER stress in several cell types.[13] However, JNK phosphorylation, indication of JNK activation, was reportedly weak in MIN6 cells even when 2 μM thapsigargin was used,[14] and we did not observe JNK phosphorylation in MIN6 cells treated with 0.5 μM thapsigargin (Figure 2B). In contrast, MIN6 cells exhibited robust phosphorylation of JNK when treated with arsenite (Figure 2B).

It is well known that 4E-BP1 is phosphorylated by mammalian target of rapamycin (mTOR). To study whether the mTOR pathway was modulated in MIN6 cells treated with arsenite, phosphorylation of ribosamal protein S6 was examined. As shown in Figure 3, together with induction of the dephosphorylated α form of 4E-BP1, arsenite dephosphorylated S6 in MIN6 cells (Figure 3), indicating

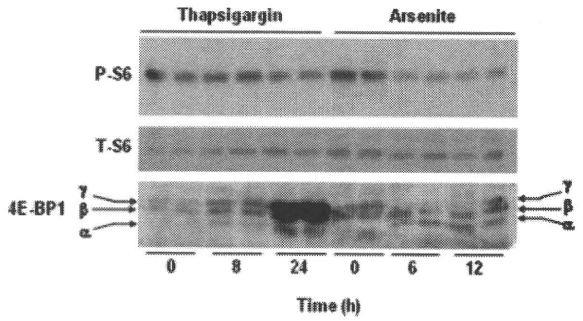

Figure 3. The mTOR pathway in MIN6 cells under ER stress or oxidative stress. Dephosphorylation of ribosomal protein S6 in MIN6 cells treated with thapsigargin (0.5 μM) or arsenite (15 μM) were examined using anti-phosphorylated S6 antibody. Western blot data shown are representative of at least three experiments

suppression of the mTOR pathway under oxidative stress conditions.

Thus, although the proximal part of the ISR was similarly activated by both ER stress and oxidative stress, expression of 4E-BP1, one of the distal branches of the ISR, was different between two stress conditions. These observations suggested that unique subpathways of the UPR and/or the oxidative stress response affected 4E-BP1 expression and/or phosphorylation. Since JNK activation was robust only in MIN6 cells exposed to an oxidative stress inducer, we speculated JNK involvement in modulation of 4E-BP1 expression under oxidative stress. Therefore, we have examined effects of a JNK inhibitor, SP600125, on 4E-BP1 expression in MIN6 cells treated with arsenite. SP600125

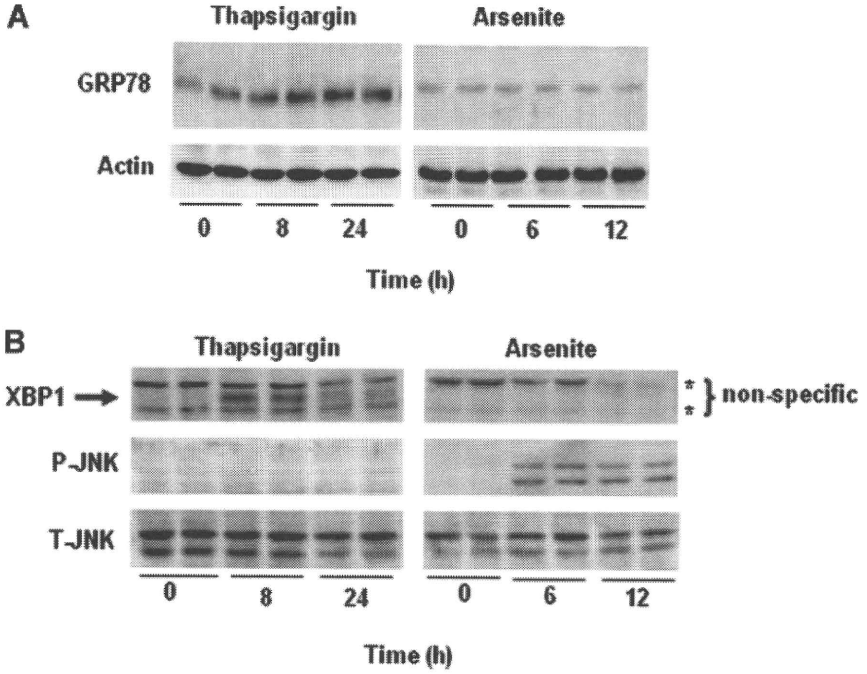

Figure 2. ATF6, IRE1/XBP1, and JNK pathways in MIN6 cells under ER stress or oxidative stress. MIN6 cells were treated with thapsigargin (0.5 μM) or arsenite (15 μM) for indicated periods, subjected to SDS-PAGE and probed with the indicated antibodies against (A) KDEL and (B) XBP1, phosphorylated JNK (P-JNK) and total JNK (T-JNK). Western blot data shown are representative of at least three experiments

treatment of MIN6 cells together with arsenite increased 4E-BP1 expression in both protein (Figure 4A) and messenger ribonucleic acid (mRNA; Figure 4B) levels. It should be noted that SP600125 did not affect thapsigargin-induced 4E-BP1 expression, ruling out direct effects on 4E-BP1 expression of the agent (data not shown). Moreover, SP600125 inhibited arsenite-induced S6 dephosphorylation, suggesting that inhibition of mTOR by arsenite is mediated at least partly via JNK activation (Figure 4A). Estimation of 4E-BP1 phosphorylation status was difficult because the total amount of 4E-BP1 was increased with SP600125 treatment. Nevertheless, quantification of ratio of the α form to the sum of β plus γ forms showed reduction in the α form of 4E-BP1 by SP600125 (Figure 4C), suggesting that JNK activation was involved in dephosphorylation of 4E-BP1 in MIN6 cells under oxidative stress conditions.

These data indicate that MIN6 cells increased total cellular 4E-BP1 activity through transcriptional induction and dephosphorylation-mediated activation under the oxidative stress conditions, while, under ER stress, MIN6 cells increased 4E-BP1 activity only through augmentation of 4E-BP1 protein levels. We have previously demonstrated that 4E-BP1 activation was important for MIN6 cell survival under ER stress conditions using 4E-BP1-deficient MIN6 cells, MIN6*Eif4ebp1*$^{-/-}$.[10] We have also tested effects on MIN6 cell survival of 4E-BP1 activation in response to arsenite challenge using the mutant cells (Figure 5). We found that the rate of MIN6 cell death was increased in MIN6*Eif4ebp1*$^{-/-}$ cells as compared to that in MIN6*WT* cells with wild-type *Eif4ebp1* alleles, suggesting that increases in 4E-BP1 activity contributed to MIN6 cell survival under oxidative stress conditions.

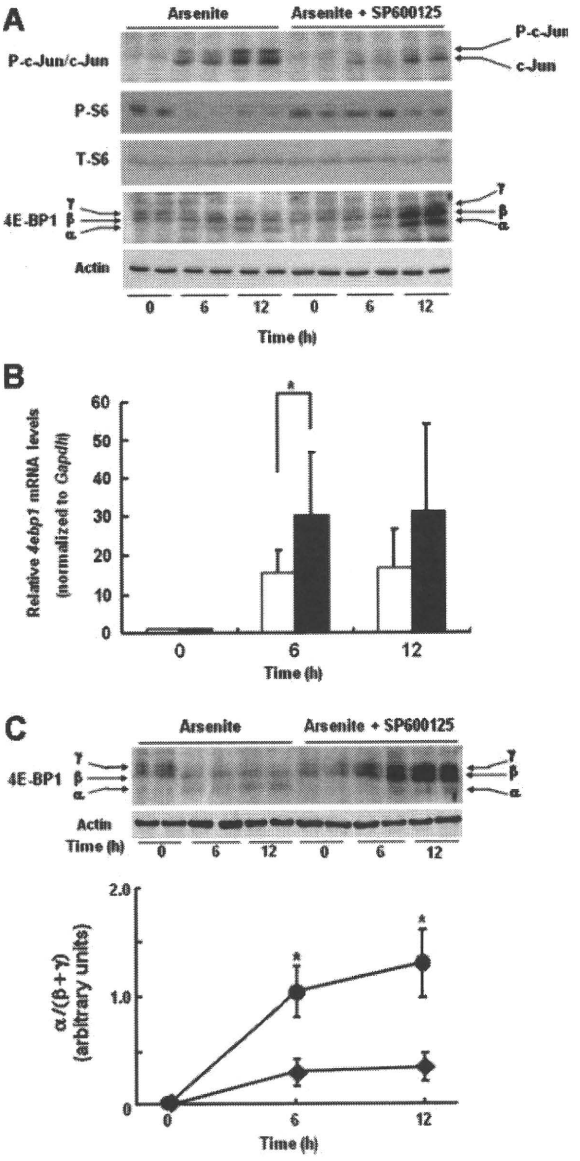

Figure 4. Involvement of JNK in oxidative stress-mediated modulation of 4E-BP1 expression and phosphorylation. (A) MIN6 cells were treated with arsenite (15 μM) in the absence or presence of SP600125 (60 μM) for 0, 6, 12 h, and expression of phosphorylated- and total S6 and 4E-BP1 protein was analyzed. Phosphorylation status of c-Jun, one of the JNK target proteins, was monitored to evaluate effectiveness of the JNK inhibitor. The experiment was repeated at least three times and similar results were obtained. (B) Total RNA was isolated from MIN6 cells treated with arsenite (15 μM) in the absence (open bars) or presence (closed bars) of SP600125 (60 μM) for 0, 6, 12 h. Relative mRNA levels of *4ebp1* transcript were obtained after normalization to *Gapdh* mRNA levels. $n = 3$, $^{*}p < 0.05$. (C) MIN6 cells were treated as in (B) and expression of phosphorylated- and non-phosphorylated 4E-BP1 protein was analyzed. The experiment was repeated three times and similar results were obtained. The intensities of three forms of 4E-BP1 bands induced by arsenite in the absence (closed circles) or presence (closed diamonds) of SP600125 were quantified and the ratio of the α form to the sum of β and γ forms are shown in the bottom ($n = 3$), $^{*}p < 0.05$

DISCUSSION

In this study, we demonstrated that 4E-BP1 was induced and contributed to survival in MIN6 pancreatic β-cells under oxidative stress conditions. While ATF4, an upstream activator of 4E-BP1 transcription was similarly induced by ER stress and oxidative stress, 4E-BP1 expression was lower with arsenite treatment than with thapsigargin. In addition, 4E-BP1 dephosphorylation was observed with arsenite treatment. Using a JNK specific inhibitor, we showed that arsenite activates JNK and modulates 4E-BP1 expression and phosphorylation.

Pancreatic β-cells are vulnerable to a variety of stress conditions.[3–5] The ISR is the common adaptive response pathway under stress conditions. We found that proximal part of the ISR was similarly activated by ER stress and oxidative stress stimuli, but that its distal part differs depending on the nature of stress stimuli. JNK activation appears to be involved in different 4E-BP1 expression and/or phosphorylation. It has been reported that ERK and p38 inhibited 4E-BP1 expression, while hyperosmorolarity-induced activation of JNK caused no changes in 4E-BP1 expression in UT7D1 cells.[15] Thus, roles of JNK on 4E-BP1 expression may be cell-type dependent, but JNK activation

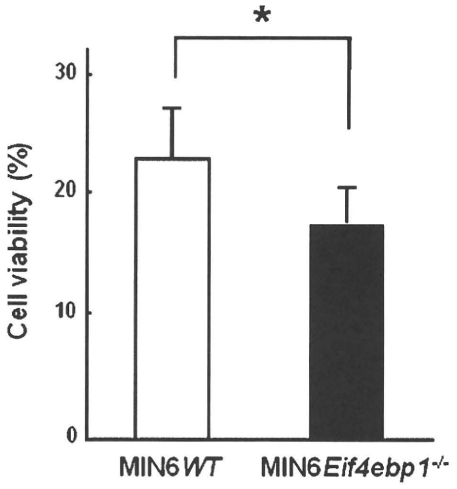

Figure 5. 4E-BP1-deficient cells exhibited increased susceptibility to oxidative stress. Viability of MIN6*WT* and MIN6*Eif4ebp1*$^{-/-}$ cells treated with 15 μM arsenite for 6 h, normalized to vehicle. $n = 8$ experiments

seems to antagonize ATF4-mediated induction of 4E-BP1 in MIN6 pancreatic β-cells.

In addition, JNK activation mediates 4E-BP1 dephosphorylation. Thus, JNK could inhibit translational initiation. Contrary, JNK inhibited 4E-BP1 transcription, possibly causing an increase in protein synthesis via reduction of the translational suppression. Therefore, JNK exerts opposing effects on protein synthesis through transcriptional suppression and dephosphorylation of 4E-BP1. The complex regulation of 4E-BP1 activity may contribute to fine tuning of translation rates under oxidative stress conditions. Regulation of 4E-BP1 activity via the ISR and JNK activation is summarized in Figure 6.

JNK activation is not observed in our MIN6 cells treated with 0.5 μM thapsigargin for up to 24 h. The same condition of ER stress caused JNK phosphorylation in mouse embryonic fibroblasts in our hands (data not shown). Therefore, ER stress-mediated JNK activation appears to vary among cell types. JNK is demonstrated to be activated by IRE1 activation in rat pancreatic acinar AR42J cells.[13] Recent studies revealed that IRE1α not only splices precursor XBP1 mRNA but also initiate variety signaling pathways through the association of adaptor proteins.[16] Pancreatic β-cells or MIN6 cells may differ from other cell types, including MEF and AR42J cells, in expression levels of such adaptor proteins, contributing to cell-type specific responses of the IRE1 pathway.

4E-BP1 plays an important role in cellular growth, differentiation, survival, and apoptosis. Although the control of 4E-BP1 activity via phosphorylation has been extensively examined, the study on mechanisms for 4E-BP1 gene expression began recently.[15,17,18] Present data, demonstrating that the JNK signaling pathway plays a role in regulation of 4E-BP1 transcription, add important information on molecular mechanisms of transcriptional control of 4E-BP1 expression and its role in stress responses.

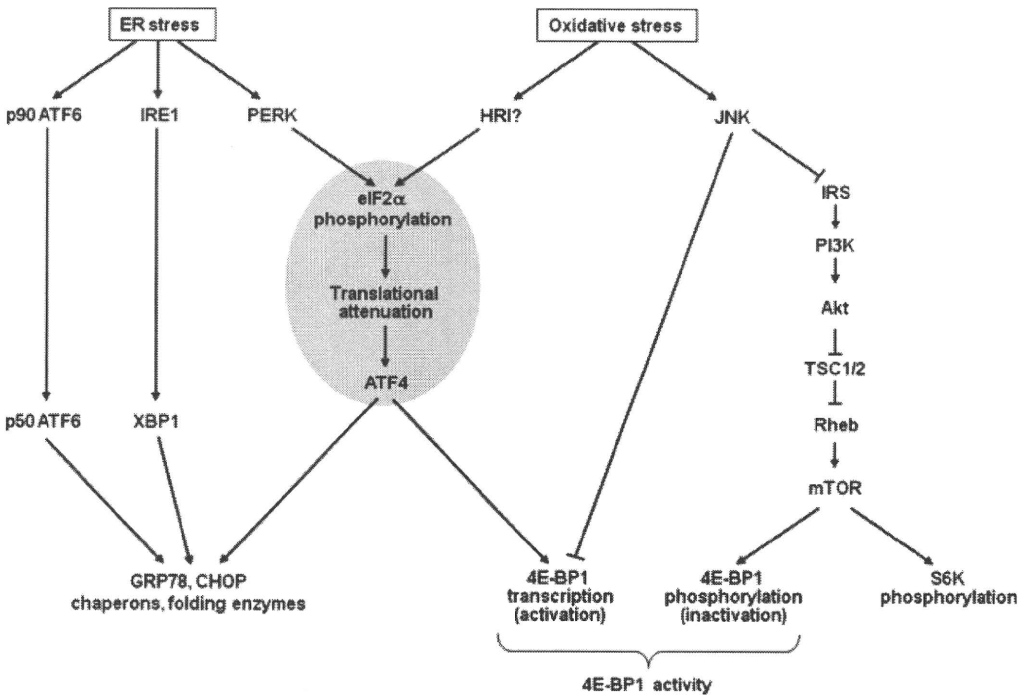

Figure 6. The ISR pathway and the PI3K/Akt/mTOR pathway converge to regulate 4E-BP1 activity under oxidative stress conditions. ER stress activates three ER resident transmembrane proteins, ATF6, IRE1, and PERK. PERK activation induces eIF2α phosphorylation, initiating the ISR (shaded area). Oxidative stress also activates the ISR, via some eIF2α kinases depending on source of oxidative stress. ATF4 activated through the ISR induces 4E-BP1 transcription. Oxidative stress-activated JNK suppresses the PI3K/Akt/mTOR pathway, dephosphorylating and activating 4E-BP1. Simultaneously, JNK suppresses transcription of 4E-BP1

CONFLICT OF INTEREST

None known.

ACKNOWLEDGEMENTS

We are grateful to C. Suzuki and M. Kato for their expert technical assistance. This research was supported by Grants-in-Aid for Scientific Research (H16-genome-003) from the Ministry of Education, Science, Sports and Culture of Japan and by 21st Global COR Program to Y.O. This work was also supported by Grants-in-Aid for Scientific Research (21591147) from the Ministry of Education, Science, Sports and Culture of Japan and a research grant from Takeda Science Foundation to H.I.

REFERENCES

1. Butler AE, Janson J, Bonner-Weir S, *et al.* Beta-cell deficit and increased beta-cell apoptosis in humans with type 2 diabetes. *Diabetes* 2003; **52**: 102–110.
2. Rahier J, Guiot Y, Goebbels RM, *et al.* Pancreatic beta-cell mass in European subjects with type 2 diabetes. *Diabetes Obes Metab* 2008; **10** (Suppl 4): 32–42.
3. Eizirik DL, Cardozo AK, Cnop M. The role for endoplasmic reticulum stress in diabetes mellitus. *Endocr Rev* 2008; **29**: 42–61.
4. Lenzen S, Drinkgrn J, Tiedge M. Low antioxidant enzyme gene expression in pancreatic islets compared other mouse tissues. *Free Radic Biol Med* 1996; **20**: 463–466.
5. Vasir B, Aiello LP, Yoon KH, *et al.* Hypoxia induces vascular endothelial growth factor gene and protein expression in cultured rat islet cells. *Diabetes* 1998; **47**: 1894–1903.
6. Malhotra JD, Kaufman RJ. Endoplasmic reticulum stress and oxidative stress: a vicious cycle or a double-edged sword? *Antioxid Redox Signal* 2007; **9**: 2277–2293.
7. Holcik M, Sonenberg N. Translational control in stress and apoptosis. *Nat Rev Mol Cell Biol* 2005; **6**: 318–327.
8. Harding HP, Zhang Y, Zeng H, *et al.* An integrated stress response regulates amino acid metabolism and resistance to oxidative stress. *Mol Cell* 2003; **11**: 619–633.
9. Proud CG. eIF2 and the control of cell physiology. *Semin Cell Dev Biol* 2005; **16**: 3–12.
10. Yamaguchi S, Ishihara H, Yamada T, *et al.* ATF4-mediated induction of 4E-BP1 contributes to pancreatic β cell survival under endoplasmic reticulum stress. *Cell Metab* 2008; **7**: 269–276.
11. Robertson RP, Harmon JS. Pancreatic islet beta-cell and oxidative stress: the importance of glutathione peroxidase. *FEBS Lett* 2007; **581**: 3743–3748.
12. Roybal CN, Hunsaker LA, Barbash O, *et al.* The oxidative stressor arsenite activates vascular endothelial growth factor mRNA transcription by an ATF4-dependent Mechanism. *J Biol Chem* 2005; **280**: 20331–20339.
13. Urano F, Wang X, Bertolotti A, *et al.* Coupling of stress in the ER to activation of JNK protein kinases by transmembrane protein kinase IRE1. *Science* 2000; **287**: 664–666.
14. Kumagai Y, Sumi D. Arsenic: Signal transduction, transcription factor, and biotransformation involved in cellular response and toxicity. *Annu Rev Pharmacol Toxicol* 2007; **47**: 243–262.
15. Rolli-Derkinderen M, Machavoine F, Baraban JM, *et al.* ERK and p38 inhibit the expression of 4E-BP1 repressor of translation through induction of Egr-1. *J Biol Chem* 2003; **278**: 18859–18867.
16. Hetz C, Glimcher LH. Fine-tuning of the unfolded protein response: assembling the IRE1alpha interactome. *Mol Cell* 2009; **35**: 551–561.
17. Stephenson AH, Seidel ER. Analysis of the interactions of Nrf-2, PMF-1, and CSN-7 with the 5′-flanking sequence of the mouse 4E-BP1 gene. *Life Sci* 2006; **79**: 1221–1227.
18. Azar R, Najib S, Lahlou H, *et al.* Phosphatidylinositol 3-kinase-dependent transcriptional silencing of the translational repressor 4E-BP1. *Cell Mol Life Sci* 2008; **65**: 3110–3117.

Hypertension Research (2010) 33, 937–943

www.nature.com/hr

ORIGINAL ARTICLE

Relationship of dysregulation of glucose metabolism with white-coat hypertension: the Ohasama study

Miki Hosaka[1], Akira Mimura[1,2], Kei Asayama[1], Takayoshi Ohkubo[1,3], Katsuhisa Hayashi[4], Masahiro Kikuya[1], Michihiro Sato[1], Takanao Hashimoto[4], Atsuhiro Kanno[4], Azusa Hara[4], Taku Obara[4,5], Hirohito Metoki[6], Ryusuke Inoue[7], Haruhisa Hoshi[8], Hiroshi Satoh[9], Yoshitomo Oka[10] and Yutaka Imai[1]

Characteristics of glucose metabolism in subjects with white-coat hypertension (WCHT) have not been fully investigated. The purpose of this study was to determine the relationship between glucose metabolism and WCHT on the basis of blood pressure (BP) at home (HBP) in the general population. Participants were from Ohasama, a rural Japanese community, and included 466 residents (mean age, 61.0 years) who had no history of diabetes mellitus. HBP and oral glucose tolerance test values were measured. Participants were classified into four groups on the basis of their HBP and casual-screening BP (CBP) values: normotension (NT) (HBP < 135/85 mm Hg, CBP < 140/90 mm Hg); WCHT (HBP < 135/85 mm Hg, CBP ⩾ 140/90 mm Hg); masked hypertension (HBP ⩾ 135/85 mm Hg, CBP < 140/90 mm Hg); or sustained hypertension (SHT) (HBP ⩾ 135/85 mm Hg, CBP ⩾ 140/90 mm Hg). The relationships between glucose metabolism and BP among the four groups were examined using multivariate analysis adjusted for possible confounding factors. Factors in relation to glucose metabolism, such as fasting glucose level, 2-h postchallenge glucose level and homeostasis model assessment-insulin resistance index, were significantly higher in subjects with WCHT and SHT than in those with NT (all $P<0.03$). When men and women were analyzed separately, these relationships were more pronounced in women. Our results suggest that dysregulation of glucose metabolism in WCHT might contribute to the increase in the long-term cardiovascular risk among the general population.
Hypertension Research (2010) **33,** 937–943; doi:10.1038/hr.2010.114; published online 15 July 2010

Keywords: general population; glucose metabolism; home blood pressure; oral glucose tolerance test; white-coat hypertension

INTRODUCTION

Self-measurement of blood pressure (BP) at home (HBP) has been recognized as a useful tool for accurate diagnosis and treatment of hypertension. Previous reports have indicated that HBP is correlated with target-organ damage, and predict the prognosis of hypertension better than casual-screening BP (CBP).[1,2]

The measurement of BP outside medical settings has identified a subgroup of individuals with white-coat hypertension (WCHT)[3] who have persistently elevated CBP but normal HBP or ambulatory BP (ABP) levels, and a subgroup of individuals with masked hypertension (MHT)[4] who have normal CBP but elevated HBP or ambulatory BP levels. The clinical significance of WCHT in relation to cardiovascular disease risk is controversial.[5,6] Similarly, there is little conclusive evidence about the association between WCHT and metabolic abnormalities.[7]

Oral glucose tolerance test (OGTT) is widely used for diagnosing diabetes mellitus (DM). Fasting glucose level is insufficient to diagnose DM; however, measuring glucose level 2-h after an oral glucose load has strong predictive power for cardiovascular disease.[8–10] Although several studies have shown the association between OGTT and CBP,[11,12] the association between OGTT and HBP remains unclear. Moreover, the relationship of WCHT and MHT with glucose metabolism is undetermined. Therefore, the aim of this study was to determine the relationship between glucose metabolism and WCHT, as well as MHT on the basis of HBP in the general population.

[1]Department of Planning for Drug Development and Clinical Evaluation, Tohoku University Graduate School of Pharmaceutical Sciences, Sendai, Japan; [2]Laboratory of Oncology, Pharmacy Practice and Sciences, Tohoku University Graduate School of Pharmaceutical Sciences, Sendai, Japan; [3]Department of Health Science, Shiga University of Medical Science, Otsu, Japan; [4]Department of Clinical Pharmacology and Therapeutics, Tohoku University Graduate School of Pharmaceutical Sciences and Medicine, Sendai, Japan; [5]Department of Pharmaceutical Sciences, Tohoku University Hospital, Sendai, Japan; [6]Department of Obstetrics and Gynecology, Tohoku University Graduate School of Medicine, Sendai, Japan; [7]Department of Medical Informatics, Tohoku University Graduate School of Medicine, Sendai, Japan; [8]Ohasama Hospital, Hanamaki, Japan; [9]Department of Environmental Health Sciences, Tohoku University Graduate School of Medicine, Sendai, Japan and [10]Department of Molecular Metabolism and Diabetes, Tohoku University Graduate School of Medicine, Sendai, Japan
Correspondence: Dr K Asayama, Department of Planning for Drug Development and Clinical Evaluation, Tohoku University Graduate School of Pharmaceutical Sciences, 6-3 Aramaki-aza-aoba, Aoba-ku, Sendai 980-8578, Japan.
E-mail: kei@asayama.org
Received 19 February 2010; revised 20 April 2010; accepted 26 April 2010; published online 15 July 2010

METHODS

Study population

This investigation is a part of a longitudinal observational study of HBP measurements among Ohasama residents that started in 1987. The socio-economic and demographic characteristics of this region and full details of the project have been described elsewhere.[13] Between 2000 and 2008, we contacted all 4809 individuals aged ⩾35 years in four districts of Ohasama town. Those who were not at home during the normal working hours of the study nurses (n=1298) and those hospitalized (n=192) or incapacitated (n=120) were not eligible. Of the remaining 3199 residents, 2181 (68%) gave written, informed consent to participate in the HBP measurement program. Of those, 700 individuals (19%) voluntarily participated in the OGTT. We excluded those treated with antidiabetic (n=11) and antihypertensive agents (n=223) from this analysis. The total number of participants statistically analyzed was thus 466. The study protocol was approved by the Institutional Review Board of Tohoku University School of Medicine, Sendai, Japan, and by the Department of Health of the Ohasama Town Government.

BP measurement

HBP was measured using the semi-automatic HEM-747IC-N or HEM701C (Omron Healthcare, Kyoto, Japan), a device based on the cuff-oscillometric method that generates a digital display of both systolic and diastolic BP values.[14] Physicians and public health nurses instructed the participants on how to use the device and record HBP results. The participants then measured their own BP once in the morning, in the sitting position within 1 h after awaking and after 2 min of rest and recorded such measurements for 4 weeks. Although many participants measured their HBP values twice or more per occasion, we used the first value from each measurement in our analysis to exclude individual selection bias.[15] HBP was defined as the mean of all measurements. The mean number of total HBP measurements was 24. CBP measurements were taken after at least 2 min of rest, twice consecutively, using an automatic device (HEM-907, Omron Healthcare) before OGTT. The average of two consecutive readings from each individual was used as CBP. The HBP and CBP measuring devices used in this study have been validated[14,16,17] and meet the criteria established by the Association for the Advancement of Medical Instrumentation.[18]

OGTT and other information

OGTT was carried out using a 75-g glucose-equivalent carbohydrate load (Trelan G; Ajinomoto Pharma, Tokyo, Japan) after the fasting blood samples were collected. Blood samples were drawn at 60 min (1 h) and 120 min (2 h), and glucose levels and insulin were measured. Information on the use of antihypertensive, hyperlipidemic and diabetic medications at baseline was obtained from interviews conducted at the time of OGTT, from records of annual health checkups and from records of Ohasama Hospital. Serum adiponectin was measured using a latex particle-enhanced turbidimetric immunoassay (SRL, Tokyo, Japan).

Classification of groups

Participants were classified into four groups (normotension (NT), WCHT, MHT and sustained hypertension (SHT)) on the basis of their HBP and CBP levels: NT, with systolic CBP < 140 mm Hg and diastolic CBP < 90 mm Hg, and systolic HBP < 135 mm Hg and diastolic HBP < 85 mm Hg; WCHT, with systolic CBP ⩾ 140 mm Hg or diastolic CBP ⩾ 90 mm Hg or both, and systolic HBP < 135 mm Hg and diastolic HBP < 85 mm Hg; MHT, with systolic CBP < 140 mm Hg and diastolic CBP < 90 mm Hg, and systolic HBP ⩾ 135 mm Hg or diastolic HBP ⩾ 85 mm Hg or both; and SHT, with systolic CBP ⩾ 140 mm Hg or diastolic CBP ⩾ 90 mm Hg or both, and systolic HBP ⩾ 135 mm Hg or diastolic HBP ⩾ 85 mm Hg or both (Figure 1). Cutoff values were derived from several guidelines.[19–21]

On the basis of OGTT, subjects were classified as having DM, impaired glucose intolerance, impaired fasting glucose or normal glucose tolerance according to the World Health Organization classification[22] (Figure 2).

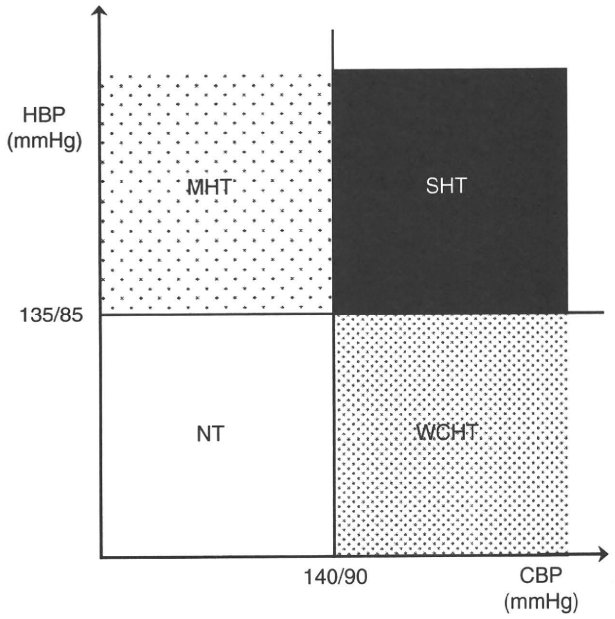

Figure 1 Distribution of subjects classified into four groups on the basis of HBP and CBP levels. CBP, casual-screening blood pressure; HBP, home blood pressure; MHT, masked hypertension; NT, normotension; SHT, sustained hypertension; WCHT, white-coat hypertension.

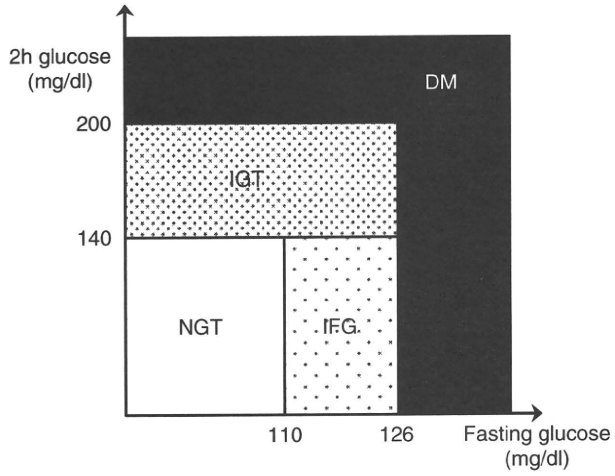

Figure 2 Distribution of subjects classified into four groups on the basis of fasting glucose and 2-h glucose level, which were determined by OGTT. DM, diabetes mellitus; IFG, impaired fasting glucose; IGT, impaired glucose tolerance; NGT, normal glucose tolerance.

Data analysis

Dyslipidemia was defined in accordance with criteria of the Japanese metabolic syndrome[23] as low high-density lipoprotein-cholesterol (<40 mg per 100 ml (1.03 mmol l^{-1})), high triglyceride (⩾150 mg per 100 ml (1.68 mmol l^{-1})) and/or the use of antilipidemic treatment. Area under the blood concentration time curve was calculated using fasting plasma glucose, 1-h glucose and 2-h glucose by quadrature by parts (area under the blood concentration time curve=(fasting plasma glucose+1-h glucose)×0.5+(1-h glucose+2-h glucose)×0.5). The homeostasis model assessment-insulin resistance index (HOMA-IR) was calculated using the following formula: HOMA-IR=fasting glucose (mg per 100 ml)×fasting insulin (μUnits per ml)/405. Insulin sensitivity was determined by the Matsuda DeFronzo index based on the following formula: 10 000/sqrt (fasting glucose (mg per 100 ml)×fasting insulin (μUnits per ml)) (mean glucose (mg per 100 ml)×mean insulin (μUnits per ml)).[24]

All data are expressed as means ± s.d. Variables were compared using Fisher's exact test, ANOVA (analysis of variance) or ANCOVA (analysis of covariance), followed by Tukey's multiple comparison test. Associations between indices for glucose metabolism and BPs as continuous variables were examined with multiple regression analysis adjusted by age, body mass index, dyslipidemia, history of cardiovascular disease, drinking habit and smoking habit. Statistical significance was established at $P<0.05$. All statistical calculations were carried out using the SAS system (version 9.1, SAS Institute, Cary, NC, USA).

RESULTS

The characteristics of the study participants are given in Table 1. The mean age was 61.0 ± 9.6 years and the proportion of men and women was 29:71. Mean systolic/diastolic CBP and HBP values were 131.3 ± 18.3/76.1 ± 11.2 mm Hg and 122.3 ± 15.0/74.5 ± 9.0 mm Hg, respectively. Of the 466 subjects, 268 were classified as having NT, 49 were classified as having MHT, 90 were classified as having WCHT and the remaining 59 were classified as having SHT. Both CBP and HBP values in the NT group were significantly lower those in than the other groups. Subjects in the NT group tended to be younger than those in the other categories of BP classification.

The relationships between glucose metabolism and each BP group were analyzed using ANCOVA (Table 2). Among subjects with WCHT and SHT, significantly higher glucose levels and HOMA-IR values and significantly lower Matsuda DeFronzo index values were observed when compared with NT (all $P<0.03$). Among those with MHT, there were no indices for glucose metabolism, which showed significant

Table 1 Characteristics of study participants

	All subjects	*Subjects with NT*	*Subjects with MHT*	*Subjects with WCHT*	*Subjects with SHT*	*ANOVA P-value*
Number of subjects (*n*)	466	268	49	90	59	—
Gender (women, %)	71.0	77.2	49.0	76.7	52.5	<0.0001
Age (years)	61.0 ± 9.6	59.8 ± 9.7	63.4 ± 9.7	62.4 ± 8.7	62.4 ± 10.0	0.02
Body mass index (kg m^{-2})	23.3 ± 3.2	22.7 ± 3.0	24.0 ± 3.6*	23.5 ± 2.8	24.9 ± 3.6*,‡	<0.0001
Height (cm)	55.6 ± 10.3	54.1 ± 9.2	59.6 ± 13.9	54.6 ± 8.7†	60.2 ± 11.6	0.02
Weight (kg)	154.2 ± 8.5	154.1 ± 8.1	156.8 ± 10.4*	152.3 ± 7.9†	155.2 ± 8.8*,‡	<0.0001
Systolic HBP (mm Hg)	122.3 ± 15.0	114.4 ± 10.7	139.5 ± 8.9*	122.5 ± 8.5*,†	143.4 ± 10.3*,‡	<0.0001
Diastolic HBP (mm Hg)	74.5 ± 9.0	70.3 ± 6.9	84.6 ± 6.8*	74.3 ± 5.7*,†	85.4 ± 7.1*,‡	<0.0001
Home heart rate (b.p.m.)	65.2 ± 7.7	64.6 ± 7.1	66.9 ± 8.1	66.1 ± 7.6	64.9 ± 9.5	0.2
Systolic CBP (mm Hg)	131.3 ± 18.3	120.8 ± 12.2	127.1 ± 9.2*	149.4 ± 9.1*,†	154.5 ± 14.4*,†,‡	<0.0001
Diastolic CBP (mm Hg)	76.1 ± 11.2	70.6 ± 8.5	75.5 ± 7.8*	85.2 ± 9.3*,†	87.7 ± 9.5*,†	<0.0001
HDL (mg per 100 ml)	62.3 ± 15.4	63.0 ± 16.0	59.2 ± 14.8	62.5 ± 14.2	61.6 ± 14.8	0.4
Triglyceride (mg per 100 ml)	100.3 ± 62.5	89.8 ± 52.7	115.6 ± 63.5*	109.1 ± 74.4	122.1 ± 73.5*	0.0002
Drinking habit (%)	41.9	40.7	59.2	26.7	55.9	0.0002
Smoking habit (%)	13.7	12.3	30.6	7.8	15.3	0.004
Dyslipidemia (%)	19.1	15.3	28.6	18.9	28.8	0.03
[a]IFG(%)	5.4	2.2	6.1	11.1	10.2	0.002
[a]IGT(%)	20.0	17.2	18.4	24.4	27.1	0.2
[a]Diabetes mellitus (%)	6.9	3.7	6.1	8.9	18.6	0.001
Past history of CVD (%)	2.8	1.9	8.2	1.1	5.1	0.04

Abbreviations: ANOVA, analysis of variance; CBP, casual-screening blood pressure; CVD, cardiovascular disease; HBP, home blood pressure; HDL, high-density lipoprotein; IFG, impaired fasting glucose; IGT, impaired glucose intolerance; MHT, masked hypertension; NT, normotension; SHT, sustained hypertension; WCHT, white-coat hypertension.
*$P<0.05$ compared with NT.
†$P<0.05$ compared with MHT.
‡$P<0.05$ compared with WCHT.
[a]IFG, IGT and diabetes mellitus were defined by the oral glucose tolerance test.

Table 2 Variables in relation to glucose metabolism

	All subjects	*Subjects with NT*	*Subjects with MHT*	*Subjects with WCHT*	*Subjects with SHT*	*ANCOVA P-value*
Number of subjects (*n*)	466	268	49	90	59	—
Fasting plasma glucose (mg per 100 ml)	95.1 ± 10.9	93.0 ± 9.7	95.1 ± 10.3	98.7 ± 12.3*	99.1 ± 11.9*	0.0003
One-hour glucose (mg per 100 ml)	157.1 ± 52.6	148.0 ± 51.0	156.2 ± 44.1	171.4 ± 49.1*	177.7 ± 61.4*	0.001
Two-hour glucose (mg per 100 ml)	126.7 ± 43.1	119.7 ± 37.6	121.6 ± 39.3	136.8 ± 50.1*	146.9 ± 49.4*,†	0.0007
Glucose AUC_{0-120} (mg per 100 ml h)	268.0 ± 71.5	254.3 ± 67.1	264.6 ± 60.3	289.2 ± 71.0*	300.7 ± 82.6*,†	0.0002
Δ60 glucose (mg per 100 ml h)	62.0 ± 48.0	55.0 ± 47.2	61.0 ± 39.3	72.7 ± 44.6*	78.6 ± 56.6*	0.01
Δ120 glucose (mg per 100 ml h)	31.6 ± 39.3	26.7 ± 34.5	26.5 ± 36.8	38.1 ± 45.1	47.9 ± 46.7*,†	0.008
HOMA	1.32 ± 0.86	1.20 ± 0.71	1.33 ± 1.09	1.47 ± 0.81*	1.66 ± 1.15*	0.03
MDI	8.89 ± 4.54	9.68 ± 4.87	9.53 ± 4.78	7.25 ± 3.13*,†	7.26 ± 3.54*,†	0.0009

Abbreviations: ANCOVA, analysis of covariance; AUC_{0-120}, area under the blood concentration time curve; HOMA, homeostasis model assessment; MDI, Matsuda DeFronzo index; MHT, masked hypertension; NT, normotension; SHT, sustained hypertension; WCHT, white-coat hypertension.
Adjusted for sex, age, body mass index, dyslipidemia, history of cardiovascular disease, drinking habit and smoking habit.
Δ60 glucose=1-h glucose—fasting plasma glucose; Δ120 glucose=2-h glucose—fasting plasma glucose.
*$P<0.05$ compared with NT.
†$P<0.05$ compared with MHT.

Table 3 Variables in relation to glucose metabolism according to sex

	All subjects	*Subjects with NT*	*Subjects with MHT*	*Subjects with WCHT*	*Subjects with SHT*	*ANCOVA P-value*
Men						
Number of subjects (*n*)	135	61	25	21	28	
Age (years)	61.2±9.1	61.0±9.4	59.2±8.7	63.8±6.2	61.5±10.6	0.4
Fasting plasma glucose (mg per 100 ml)	97.4±10.9	96.1±10.4	96.2±12.4	98.5±8.4	100.5±11.9	0.6
One-hour glucose (mg per 100 ml)	168.5±58.5	164.7±61.5	164.5±48.5	165.2±52.3	182.6±64.9	0.7
Two-hour glucose (mg per 100 ml)	129.0±47.4	124.9±46.8	130.2±44.4	124.6±39.4	140.1±56.4	0.7
Glucose AUC_{0-120} (mg per 100 ml h)	281.7±78.2	275.2±80.8	277.7±70.0	276.8±65.1	302.9±88.0	0.7
Δ60 glucose (mg per 100 ml h)	71.1±54.2	68.7±57.9	68.2±42.3	66.7±49.2	82.0±59.9	0.8
Δ120 glucose (mg per 100 ml h)	31.6±43.6	28.9±42.2	34.0±40.8	26.1±39.4	39.6±52.1	0.8
HOMA	1.31±0.96	1.15±0.62	1.33±1.15	1.29±0.81	1.64±1.37	0.3
MDI	9.76±5.29	11.0±6.11	10.1±5.05	8.51±3.83	7.75±3.62*	0.03
Women						
Number of subjects (*n*)	331	207	24	69	31	
Age (years)	61.0±9.8	59.5±9.8	67.7±8.8*	62.0±9.3	63.3±9.5	0.0003
Fasting plasma glucose (mg per 100 ml)	94.2±10.7	92.1±9.3	94.0±7.6	98.7±13.3*	97.7±12.0*	0.0005
One-hour glucose (mg per 100 ml)	152.5±49.3	143.0±46.5	147.5±38.1	173.3±48.3*	173.2±58.7*	0.0006
Two-hour glucose (mg per 100 ml)	125.7±41.3	118.2±34.4	112.7±31.6	140.5±52.6*,†	153.1±42.1*,†	<0.0001
Glucose AUC_{0-120} (mg per 100 ml h)	262.4±67.9	248.2±61.4	250.8±45.8	292.9±72.7*	298.7±78.8*	<0.0001
Δ60 glucose (mg per 100 ml h)	58.3±44.8	50.9±42.9	53.5±35.2	74.6±43.4*	75.5±54.2*	0.005
Δ120 glucose (mg per 100 ml h)	31.5±37.5	26.1±32.0	18.7±30.9	41.8±46.3*,†	55.4±40.6*,†	0.0002
HOMA	1.33±0.81	1.21±0.74	1.33±1.04	1.52±0.82*	1.67±0.92*	0.2
MDI	8.53±4.16	9.29±4.38	8.98±4.52	6.86±2.80*	6.83±3.46*	0.3

Abbreviations: ANCOVA, analysis of covariance; AUC_{0-120}, area under the blood concentration time curve; HOMA, homeostasis model assessment; MDI, Matsuda DeFronzo index; MHT, masked hypertension; NT, normotension; SHT, sustained hypertension; WCHT, white-coat hypertension.
Adjusted for age, body mass index, dyslipidemia, history of cardiovascular disease, drinking habit and smoking habit.
Δ60 glucose=1-h glucose—fasting plasma glucose; Δ120 glucose=2-h glucose—fasting plasma glucose.
* $P<0.05$ compared with NT.
† $P<0.05$ compared with MHT.

differences from those in subjects with NT. Similarly, no significant difference was observed between subjects with WCHT and those with SHT. Further analysis in subjects in which serum adiponectin levels were measured ($n=167$) showed that significantly lower adiponectin levels were observed in subjects with WCHT (10.5±6.0) when compared with those with NT (14.7±6.7) ($P=0.044$). Similar trends were observed only in women (data not shown).

The results in which men and women were analyzed separately are shown in Table 3. There were no significant differences in fasting glucose levels, 2-h glucose levels, HOMA-IR and the Matsuda DeFronzo index between MHT and NT regardless of sex. For women with WCHT and SHT, glucose levels were significantly higher than those with NT. Meanwhile, no significant differences of glucose levels among BP groups were observed in men. HOMA-IR in women was significantly higher in individuals with WCHT and SHT (1.5±0.8 and 1.7±0.9, respectively) than in those with NT (1.2±0.7), whereas HOMA-IR in men did not differ among the four BP groups. Similar results were observed with regard to the Matsuda DeFronzo index, although the Matsuda DeFronzo index in men was significantly higher in individuals with SHT (7.7±3.6) than in those with NT (11.0±6.1). However, there was no significant interaction between BP groups and sex in relation to glucose levels, HOMA-IR and the Matsuda DeFronzo index (all $P>0.2$).

The results of multiple regression analysis indicated that CBP values were significantly associated with several indices for glucose metabolism even adjusted by confounding factors. When systolic HBP and systolic CBP values were simultaneously included in the model (Table 4), systolic CBP, but not systolic HBP, was significantly associated with indices for glucose metabolism, especially with fasting plasma glucose ($P=0.14$ for systolic HBP, $P<0.0001$ for systolic CBP).

DISCUSSION

In this study, glucose levels in subjects with WCHT and SHT were significantly higher than those with NT. In a previous study, young subjects with WCHT tended to have metabolism dysregulation.[25] In a population-based study, individuals with WCHT showed impaired insulin sensitivity compared with normotensive subjects in their late middle age.[26] Sympathetic nervous system activity has been associated with the development of WCHT and with insulin resistance.[27,28] Furthermore, CBP values were reported to be positively correlated with HOMA-IR.[29] Central sympathetic hyperactivity has also reported to exist in WCHT in the clinical setting.[27] Although we have not investigated sympathetic nerve activities in this study, the strong relationship between CBP and glucose metabolisms would support the existence of sympathetic nervous system hyperactivity in individuals with WCHT and SHT.

In this study, significant correlations between glucose dysregulation and WCHT were not observed in men. Sympathetic nerve activity would differ between men and women with WCHT. However, to our knowledge, there was no previous study about the sympathetic nerve system for difference between men and women with WCHT. Thus we cannot explain this difference between men and women from the viewpoint of the sympathetic nerve system. Other factors would contribute to hyperglycemia in individuals with WCHT, whereas the result might be just by chance because of a small number of participants. The difference between men and women should be investigated on the basis of a large population.

Table 4 Independent relations between indices for glucose metabolism and BP as determined by multiple regression analysis

	HBP		*CBP*		*Sex*		*Age*		*BMI*		*Dyslipidemia*		*Drinking habit*		*Smoking habit*		
	β	*s.e.*	*β*	*s.e.*	*β*	*s.e.*	*β*	*s.e.*	*β*	*s.e.*	*β*	*s.e.*	*β*	*s.e.*	*β*	*s.e.*	R^2
Fasting plasma glucose (mg per 100 ml)	−0.060	0.040	0.168	0.031‡	2.180	1.364	0.116	0.06*	0.385	0.164*	1.406	1.274	−1.150	1.157*	−0.170	1.651	0.1227
One-hour glucose (mg per 100 ml)	0.094	0.198	0.416	0.152*	12.630	6.696	0.830	0.27†	0.880	0.806	8.043	6.254	4.134	5.682	−6.550	8.105	0.0962
Two-hour glucose (mg per 100 ml)	0.191	0.163	0.346	0.125*	4.129	5.513	0.348	0.22	1.533	0.664*	6.960	5.149	4.184	4.678	5.757	6.673	0.0899
Glucose AUC $_{0\text{-}120}$ (mg per 100 ml h)	0.160	0.267	0.673	0.205†	15.790	9.029	1.062	0.37†	1.839	1.087	12.230	8.432	5.650	7.661	−3.760	10.930	0.1112
Δ60 glucose (mg per 100 ml h)	0.153	0.183	0.248	0.140	10.460	6.187	0.714	0.25†	0.495	0.745	6.637	5.779	5.286	5.250	−6.380	7.489	0.0749
Δ120 glucose (mg per 100 ml h)	0.251	0.150	0.178	0.116	1.949	5.093	0.232	0.21	1.149	0.613	5.554	4.756	5.336	4.321	5.929	6.164	0.0640
HOMA	0.002	0.003	0.004	0.002	−0.030	0.103	−0.010	0†	0.090	0.012‡	0.226	0.096*	0.146	0.087	−0.050	0.125	0.1949
MDI	−0.010	0.016	−0.040	0.012†	0.332	0.529	0.019	0.02	−0.470	0.064‡	−1.440	0.494†	−1.570	0.449†	−1.330	0.640*	0.2459
[a]Adiponectin (μg ml^{-1})	−0.030	0.040	0.026	0.028	−4.730	1.239†	0.221	0.05‡	−0.740	0.146‡	−1.000	1.151	−1.030	1.025	−0.300	1.528	0.3758

Abbreviations: $AUC_{0\text{-}120}$, area under the blood concentration time curve; BMI, body mass index; BP, blood pressure; CBP, casual-screening blood pressure; HBP, home blood pressure; HOMA, homeostasis model assessment; MDI, Matsuda DeFronzo index.
*$P<0.05$, †$P<0.005$, ‡$P<0.0001$.
Δ60 glucose=1-h glucose−fasting plasma glucose; Δ120 glucose=2-h glucose−fasting plasma glucose.
[a]The number of subjects who have the data of adiponectin is 167.

The association between WCHT and the risk of cardiovascular disease is inconsistent. Although many reports have shown that the risk of cardiovascular disease in subjects with WCHT was comparable with NT,[6,30] our previous report indicated that WCHT is correlated with high risk for development of SHT and suggested that WCHT would carry a poor cardiovascular prognosis on a long-term basis.[31] The cumulative hazard for stroke in the WCHT group was equal to that of the ambulatory hypertensive group according to the results of a meta-analysis of prospective studies, including the Ohasama study.[32] Thus, dysregulation of glucose metabolism might be associated with WCHT, which is a risk factor for cardiovascular disease in the long term. Diabetic nephropathy and diabetic retinopathy were more progressive in diabetic individuals with WCHT than in those with NT.[33] It would be useful for individuals with WCHT to undergo an OGTT to detect dysregulation of glucose metabolism in the early stages. Furthermore, early detection and prevention for progression from WCHT to SHT should be monitored by consecutive measurements of HBP.

Significantly low adiponectin levels were observed in subjects with WCHT compared with those with NT. The observations also support the involvement of insulin resistance in glucose dysmetabolism. The role of adipocytokine might explain sex differences for glucose metabolism as this tendency was observed especially in women; however, the number of subjects was very small especially when men and women were analyzed separately. The association between adipocytokine or sex difference and glucose metabolism should be investigated with a large number of participants.

No significant difference in indices for glucose metabolism was observed between subjects with WCHT and those with SHT. However, the tendency of low adiponectin levels was observed in subjects with WCHT compared with those with SHT. Although there were small (although not statistically significant) differences in indices for glucose metabolism between WCHT and SHT, significantly low weight and body mass index were observed in subjects with WCHT when compared with those with SHT. Despite this, the level of adiponectin in subjects with WCHT was lower and the level of glucose metabolism dysregulation was comparable when compared with those with SHT. Thus, we believe that WCHT is not comparable with SHT and might not be a safe condition.

There was no specific tendency for glucose metabolism in MHT in this study. In previous studies, fasting glucose levels were reported to be significantly higher in the MHT group than in the NT group, and those in the MHT group were similar to the SHT group.[7,34] These results were inconsistent with our findings that glucose metabolism of subjects with MHT was comparable with those with NT. The most likely explanation is that individuals treated with antihypertensive medication were excluded from this study. Several previous studies in relation to the prognosis of MHT consisted of subjects treated with antihypertensive medication[7,35] or included subjects both with and without antihypertensive medication.[36] Although the high risk of cerebrovascular and cardiovascular disease in subjects with MHT has been established by these previous studies, the risk for individuals with MHT without antihypertensive medication would be a separate concern. Exclusion of subjects taking antihypertensive medication in the current study resulted in an insufficient number of subjects in each BP category and might lead to insufficient statistical power to draw a conclusion. Thus, further research including individuals who use antihypertensive medication would be necessary to clarify the association between MHT and dysregulation of glucose metabolism.

It should also be noted that subjects who were previously diagnosed with DM and those treated with antidiabetic agents did not participate

in this study. Several studies including our previous study have shown that many subjects with MHT had a history of DM[37] or were prescribed antidiabetic treatment.[38,39] In this study, subjects with MHT might have been excessively excluded, and thus glucose levels of the MHT group might be underestimated and create a weak association between MHT and glucose levels. The possibility of selection bias should be considered when generalizing the report findings. Furthermore, the number of subjects with MHT (n=49) in this study was relatively small, which resulted in an insufficient statistical power; the association between MHT and the dysregulation of glucose metabolism remain a matter for debate. It is also well known that patients with MHT have a greater frequency of target-organ damage[34,37] and have a greater risk of cardiovascular disease.[36] Thus, it is important to promote further research with a large number of subjects, including those with DM to confirm the association between dysregulation of glucose metabolism and MHT.

According to the multiple regression model, CBP would be more useful for predicting dysregulation of glucose metabolism or insulin resistance than HBP. In the previous study, it was established that HBP value has a stronger predictive power for target-organ damage, morbidity and mortality than has the CBP value.[1,2] Glucose metabolism is also treated as a risk factor for cardiovascular diseases.[9,10] It seems reasonable to suppose that HBP and glucose metabolism would affect to cardiovascular diseases independently. Further follow-up studies are required to investigate long-term prognosis in terms of comparing BP information and glucose metabolism.

There were several limitations in this study. OGTT data were obtained at only one measurement in one occasion. If we carry out OGTT twice or more, the classification based on OGTT might be changed. We excluded patients with DM or with a history of DM. The study participants might not be the same as the entire population of Ohasama, and study participants' potential awareness of health concerns would be higher than the other residents in the general population. Thus, the possibility of selection bias needs to be considered when generalizing the present findings. Furthermore, this study included a comparably small number of men without data of participants' detailed lifestyle, although sex-specific associations were observed. Women have reported to have a greater tendency to be influenced by the white-coat effect than men,[40,41] and decreased glucose tolerance related to poor lifestyle choices was more common in women than in men.[42] Therefore, further prospective studies based on a sufficient number of subjects with detailed information are required to overcome these limitations.

In conclusion, strong associations between dysregulation of glucose metabolism and WCHT were observed in this study. Our findings suggest that dysregulation of glucose metabolism might contribute to the increase in the long-term risk of poor prognosis for subjects with WCHT. It is useful for individuals with WCHT to undergo OGTT to detect early stages of dysregulation of glucose metabolism. Consecutive measurements of HBP would also be important to detect and to prevent progression from WCHT to SHT.

CONFLICT OF INTEREST

The authors declare no conflict of interest.

ACKNOWLEDGEMENTS

We express our gratitude to the Ohasama public health nurses and technicians, as well as the secretarial staff of our laboratory. This study was supported in part by Grants for Scientific Research (15790293, 16590433, 17790381, 18390192, 18590587, 19590929, 19790423, 20590629, 21390201 and 21591016) from the Ministry of Education, Culture, Sports, Science, and Technology, Japan; Grant-in-Aid (H17-Kenkou-007, H18-Junkankitou (Seishuu)-Ippan-012, and H20-Junkankitou (Seishuu)-Ippan-009, 013) from the Ministry of Health, Labor and Welfare, Health and Labor Sciences Research Grants, Japan; Grant-in-Aid for Japan Society for the Promotion of Science (JSPS) fellows (16.54041, 18.54042, 19.7152, 20.7198, 20.7477 and 20.54043); Health Science Research Grants and Medical Technology Evaluation Research Grants from the Ministry of Health, Labor and Welfare, Japan; Japan Atherosclerosis Prevention Fund; Uehara Memorial Foundation; Takeda Medical Research Foundation; National Cardiovascular Research Grants; and Biomedical Innovation Grants.

1 Ohkubo T, Imai Y, Tsuji I, Nagai K, Kato J, Kikuchi N, Nishiyama A, Aihara A, Sekino M, Kikuya M, Ito S, Satoh H, Hisamichi S. Home blood pressure measurement has as stronger predictive power for mortality than dose screening blood pressure measurement: a population-based observation in Ohasama, Japan. *J Hypertens* 1998; **16**: 971–975.
2 Ohkubo T, Asayama K, Kikuya M, Metoki H, Hoshi H, Hashimoto J, Totsune K, Satoh H, Imai Y. How many times should blood pressure be measured at home for better prediction of stroke risk? Ten-year follow-up results from the Ohasama study. *J Hypertens* 2004; **22**: 1099–1104.
3 Pickering TG, James GD, Boddie C, Harshfield GA, Blank S, Laragh JH. How common is white coat hypertension? *JAMA* 1988; **259**: 225–228.
4 Pickering TG, Davidson K, Gerin W, Schwartz JE. Masked hypertension. *Hypertension* 2002; **40**: 795–796.
5 Gustavsen PH, Hoegholm A, Bang LE, Kristensen KS. White coat hypertension is a cardiovascular risk factor: a 10-year follow-up study. *J Hum Hypertens* 2003; **17**: 811–817.
6 Kario K, Shimada K, Schwartz JE, Matsuo T, Hoshide S, Pickering TG. Silent and clinically overt stroke in older Japanese subjects with white-coat and sustained hypertension. *J Am Coll Cardiol* 2001; **38**: 238–245.
7 Mancia G, Bombelli M, Facchetti R, Madotto F, Quarti-Trevano F, Grassi G, Sega R. Increased long-term risk of new-onset diabetes mellitus in white-coat and masked hypertension. *J Hypertens* 2009; **27**: 1672–1978.
8 Rodriguez BL, Lau N, Burchfiel CM, Abbott RD, Sharp DS, Yano K, Curb JD. Glucose intolerance and 23-year risk of coronary heart disease and total mortality: the Honolulu Heart Program. *Diabetes Care* 1999; **22**: 1262–1265.
9 Tominaga M, Eguchi H, Manaka H, Igarashi K, Kato T, Sekikawa A. Impaired glucose tolerance is a risk factor for cardiovascular disease, but not impaired fasting glucose. The Funagata Diabetes Study. *Diabetes Care* 1999; **22**: 920–924.
10 Nakagami T, DECODA Study Group. Hyperglycaemia and mortality from all causes and from cardiovascular disease in five populations of Asian origin. *Diabetlogia* 2004; **47**: 385–394.
11 Zhang Y, Lee ET, Devereux RB, Yeh J, Best LG, Fabsitz RR, Howard BV. Prehypertension, diabetes, and cardiovascular disease risk in a population-based sample: the Strong Heart Study. *Hypertension* 2006; **47**: 410–414.
12 Korhonen P, Aarnio P, Saaresranta T, Jaatinen P, Kantola I. Glucose homeostasis in hypertensive subjects. *Hypertension* 2008; **51**: 945–949.
13 Imai Y, Satoh H, Nagai K, Sakuma M, Sakuma H, Minami N, Munakata M, Hashimoto J, Yamagishi T, Watanabe N, Yabe T, Nishiyama A, Nakatsuka H, Koyama H, Abe K. Characteristic of a community-based distribution of home blood pressure in Ohasama in northern Japan. *J Hypertens* 1993; **11**: 1441–1449.
14 Imai Y, Abe K, Sasaki S, Minami N, Munakata M, Sakuma H, Hashimoto J, Sekino H, Imai K, Yoshinaga K. Clinical evaluation of semiautomatic and automatic devices for home blood pressure measurement: comparison between cuff-oscillometric and microphone methods. *J Hypertens* 1989; **7**: 983–990.
15 Imai Y, Otsuka K, Kawano Y, Shimada K, Hayashi H, Tochikubo O, Miyakawa M, Fukiyama K. Japanese society of hypertension (JSH) guidelines for self-monitoring of blood pressure at home. *Hypertens Res* 2003; **26**: 771–782.
16 Imai Y, Nishiyama A, Sekino M, Aihara A, Kikuya M, Ohkubo T, Matsubara M, Hozawa A, Tsuji I, Ito S, Satoh H, Nagai K, Hisamichi S. Characteristics of blood pressure measured at home in the morning and in the evening: the Ohasama study. *J Hypertens* 1999; **17**: 889–898.
17 White WB, Anwar YA. Evaluation of the overall efficacy of the Omron office digital blood pressure HEM-907 monitor in adults. *Blood Press Monit* 2001; **6**: 107–110.
18 Association for the Advancement of Medical Instrumentation. *American National Standards for Electronic or Automated Sphygmomanometers*. AAMI Analysis and Review: Washington, DC, 1987.
19 European Society of Hypertension-European Society of Cardiology Guidelines Committee. 2003 European Society of Hypertension-European Society of Cardiology guidelines for the management of arterial hypertension. *J Hypertens* 2003; **21**: 1011–1053.
20 Chobanian AV, Bakris GL, Black HR, Cushman WC, Green LA, Izzo Jr JL, Jones DW, Materson BJ, Oparil S, Wright Jr JT, Roccella EJ. The Seventh Report of the Joint National Committee on Prevention, Detection, Evaluation, and Treatment of High Blood Pressure: the JNC 7 report. *JAMA* 2003; **289**: 2560–2572.
21 Japanese Society of Hypertension. Japanese Society of Hypertension guidelines for the management of hypertension (JSH 2004). *Hypertens Res* 2006; **29**: S1–S105.
22 Alberti KG, Zimmet PZ. Definition, diagnosis and classification of diabetes mellitus and its complications. Part 1: diagnosis and classification of diabetes mellitus provisional report of a WHO consultation. *Diabet Med* 1998; **15**: 539–553.

23 Committee to Evaluate Diagnostic Standards for Metabolic Syndrome. Definition and the diagnostic standard for metabolic syndrome [in Japanese]. *Nippon Naika Gakkai Zasshi* 2005; **94**: 794–809.
24 Matsuda M, DeFronzo RA. Insulin sensitivity indices obtained from oral glucose tolerance testing: comparison with the euglycemic insulin clamp. *Diabetes Care* 1999; **22**: 1462–1470.
25 Julius S, Mejia A, Jones K, Krause L, Schork N, van de Ven C, Johnson E, Petrin J, Sekkarie MA, Kjeldsen SE. 'White coat' versus 'sustained' borderline hypertension in Tecumseh, Michigan. *Hypertension* 1990; **16**: 617–623.
26 Björklund K, Lind L, Vessby B, Andrén B, Lithell H. Different metabolic predictors of white-coat and sustained hypertension over a 20-year follow-up period: a population-based study of elderly men. *Circulation* 2002; **106**: 63–68.
27 Smith PA, Graham LN, Mackintosh AF, Stoker JB, Mary DA. Sympathetic neural mechanisms in white-coat hypertension. *J Am Coll Cardiol* 2002; **40**: 126–132.
28 Esler M, Straznicky N, Eikelis N, Masuo K, Lambert G, Lambert E. Mechanisms of sympathetic activation in obesity-related hypertension. *Hypertension* 2006; **48**: 787–796.
29 Hirose H, Saito I, Kawabe H, Saruta T. Insulin resistance and hypertension: seven-year follow-up study in middle-aged Japanese men (the KEIO study). *Hypertens Res* 2003; **26**: 795–800.
30 Khattar RS, Senior R, Lahiri A. Cardiovascular outcome in white-coat versus sustained mild hypertension: a 10-year follow-up study. *Circulation* 1998; **98**: 1892–1897.
31 Ugajin T, Hozawa A, Ohkubo T, Asayama K, Kikuya M, Obara T, Metoki H, Hoshi H, Hashimoto J, Totsune K, Satoh H, Tsuji I, Imai Y. White-coat hypertension as a risk factor for the development of home hypertension: the Ohasama study. *Arch Intern Med* 2005; **165**: 1541–1546.
32 Verdecchia P, Reboldi GP, Angeli F, Schillaci G, Schwartz JE, Pickering TG, Imai Y, Ohkubo T, Kario K. Short- and long-term incidence of stroke in white-coat hypertension. *Hypertension* 2005; **45**: 203–208.
33 Kramer CK, Leitão CB, Canani LH, Gross JL. Impact of white-coat hypertension on microvascular complications in type 2 diabetes. *Diabetes Care* 2008; **31**: 2233–2237.
34 Liu JE, Roman MJ, Pini R, Schwartz JE, Pickering TG, Devereux RB. Cardiac and arterial target organ damage in adults with elevated ambulatory and normal office blood pressure. *Ann Intern Med* 1999; **131**: 564–572.
35 Bobrie G, Chatellier G, Genes N, Clerson P, Vaur L, Vaisse B, Menard J, Mallion JM. Cardiovascular prognosis of 'masked hypertension' detected by blood pressure self-measurement in elderly treated hypertensive patients. *JAMA* 2004; **291**: 1342–1349.
36 Ohkubo T, Kikuya M, Metoki H, Asayama K, Obara T, Hashimoto J, Totsune K, Hoshi H, Satoh H, Imai Y. Prognosis of 'masked' hypertension and 'white-coat' hypertension detected by 24-h ambulatory blood pressure monitoring 10-year follow-up from the Ohasama study. *J Am Coll Cardiol* 2005; **46**: 508–515.
37 Hara A, Ohkubo T, Kikuya M, Shintani Y, Obara T, Metoki H, Inoue R, Asayama K, Hashimoto T, Harasawa T, Aono Y, Otani H, Tanaka K, Hashimoto J, Totsune K, Hoshi H, Satoh H, Imai Y. Detection of carotid atherosclerosis in individuals with masked hypertension and white-coat hypertension by self-measured blood pressure at home: the Ohasama study. *J Hypertens* 2007; **25**: 321–327.
38 Marchesi C, Maresca AM, Solbiati F, Franzetti I, Laurita E, Nicolini E, Gianni M, Guasti L, Marnini P, Venco A, Grandi AM. Masked hypertension in type 2 diabetes mellitus. Relationship with left-ventricular structure and function. *Am J Hypertens* 2007; **20**: 1079–1084.
39 Ben-Dov IZ, Ben-Ishay D, Mekler J, Ben-Arie L, Bursztyn M. Increased prevalence of masked blood pressure elevations in treated diabetic subjects. *Arch Intern Med* 2007; **22**: 2139–2142.
40 Hozawa A, Ohkubo T, Nagai K, Kikuya M, Matsubara M, Tsuji I, Ito S, Satoh H, Hisamichi S, Imai Y. Factors affecting the difference between screening and home blood pressure measurements: the Ohasama Study. *J Hypertens* 2001; **19**: 13–19.
41 Staessen JA, O'Brien ET, Atkins N, Amery AK. Short report: ambulatory blood pressure in normotensive compared with hypertensive subjects. The *Ad-Hoc* Working Group. *J Hypertens* 1993; **11**: 1289–1297.
42 Dunstan DW, Salmon J, Healy GN, Shaw JE, Jolley D, Zimmet PZ, Owen N, AusDiab Steering Committee. Association of television viewing with fasting and 2-h postchallenge plasma glucose levels in adults without diagnosed diabetes. *Diabetes Care* 2007; **30**: 516–522.

Interleukin-6 Enhances Glucose-Stimulated Insulin Secretion From Pancreatic β-Cells

Potential Involvement of the PLC-IP_3–Dependent Pathway

Toshinobu Suzuki,[1,2] Junta Imai,[2] Tetsuya Yamada,[1] Yasushi Ishigaki,[2] Keizo Kaneko,[1] Kenji Uno,[2] Yutaka Hasegawa,[2] Hisamitsu Ishihara,[2] Yoshitomo Oka,[2] and Hideki Katagiri[1]

OBJECTIVE—Interleukin-6 (IL-6) has a significant impact on glucose metabolism. However, the effects of IL-6 on insulin secretion from pancreatic β-cells are controversial. Therefore, we analyzed IL-6 effects on pancreatic β-cell functions both in vivo and in vitro.

RESEARCH DESIGN AND METHODS—First, to examine the effects of IL-6 on in vivo insulin secretion, we expressed IL-6 in the livers of mice using the adenoviral gene transfer system. In addition, using both MIN-6 cells, a murine β-cell line, and pancreatic islets isolated from mice, we analyzed the in vitro effects of IL-6 pretreatment on insulin secretion. Furthermore, using pharmacological inhibitors and small interfering RNAs, we studied the intracellular signaling pathway through which IL-6 may affect insulin secretion from MIN-6 cells.

RESULTS—Hepatic IL-6 expression raised circulating IL-6 and improved glucose tolerance due to enhancement of glucose stimulated-insulin secretion (GSIS). In addition, in both isolated pancreatic islets and MIN-6 cells, 24-h pretreatment with IL-6 significantly enhanced GSIS. Furthermore, pretreatment of MIN-6 cells with phospholipase C (PLC) inhibitors with different mechanisms of action, U-73122 and neomycin, and knockdowns of the IL-6 receptor and PLC-β_1, but not with a protein kinase A inhibitor, H-89, inhibited IL-6–induced enhancement of GSIS. An inositol triphosphate (IP_3) receptor antagonist, Xestospondin C, also abrogated the GSIS enhancement induced by IL-6.

CONCLUSIONS—The results obtained from both in vivo and in vitro experiments strongly suggest that IL-6 acts directly on pancreatic β-cells and enhances GSIS. The PLC-IP_3–dependent pathway is likely to be involved in IL-6-mediated enhancements of GSIS. ***Diabetes*** **60:537–547, 2011**

Interleukin-6 (IL-6) is a pleiotropic cytokine produced by several cell types, such as immune cells, adipocytes, myocytes, and endothelial cells. Although IL-6 was initially identified as an immuno-modulatory cytokine secreted from macrophages, several previous studies revealed that IL-6 also has significant impacts on nonimmune events (1), including glucose metabolism.

Obesity is reportedly associated with elevation of circulating IL-6 (2). Functions of IL-6 in insulin-sensitive tissues have been explored by many researchers. There is growing evidence suggesting that IL-6 exacerbates insulin resistance in the liver and adipose tissue, while improving insulin sensitivity in muscle (2). In contrast, the effect of IL-6 on insulin secretion from pancreatic β-cells remains unclear. The IL-6 receptor (IL-6R) was reportedly expressed in murine pancreatic β-cells (3), suggesting a direct impact of IL-6 on pancreatic β-cells. However, a number of controversial in vitro studies demonstrated IL-6 to increase (4,5), decrease (6–8), and have no effect on (9) insulin secretion from isolated pancreatic islets or β-cell lines.

On the other hand, two studies have recently suggested stimulatory effects of IL-6 on insulin secretion in vivo. IL-6 overexpression in muscle, using an electro-transfer method, reduced body fat with liver inflammation and decreased insulin sensitivity in muscle (10). Blood glucose was also shown to be lowered especially in fed states due to enhanced glucose-stimulated insulin secretion (GSIS) in mice, although this study was focused mainly on the liver and muscle (10). In addition, involvement of IL-6 in insulin secretion was recently reported using IL-6-deficient mice (3). High fat (HF)-fed IL-6-knockout (KO) mice displayed no pancreatic α-cell expansion and decreased glucagon levels with impaired GSIS (3). Although the effects of IL-6 on pancreatic α-cell expansion were mainly analyzed, the aforementioned finding prompted us to hypothesize that HF-induced hyperIL-6-emia enhances GSIS. Furthermore, in human subjects as well, association of the plasma IL-6 concentration with first-phase insulin secretion was reported (11). Collectively, chronic elevation of plasma IL-6 concentrations might promote insulin secretion independently of insulin resistance. Therefore, in the current study, to determine the precise role of IL-6 in pancreatic β-cell function, we performed in vivo and in vitro experiments. We first expressed IL-6 in the livers of mice using the adenoviral gene transfer system. Hepatic IL-6 expression raised circulating IL-6 levels accompanied by marked enhancements of GSIS. We also examined the in vitro effects of IL-6 pretreatment on insulin secretion from both pancreatic islets isolated from mice and MIN-6 cells, a murine β-cell line. These experiments showed GSIS enhancement. Finally, we demonstrated that the phospholipase C (PLC)-inositol triphosphate (IP_3) dependent pathway is involved in IL-6 enhancement of GSIS in pancreatic β-cells.

RESEARCH DESIGN AND METHODS

Recombinant adenoviruses. Murine IL-6 cDNA was cloned from a liver cDNA library by PCR and ligated into adenovirus vector and then transfected into 293 human embryonic kidney cells. LacZ adenovirus was used as the control (12).

From the [1]Department of Metabolic Diseases, Center for Metabolic Diseases, Tohoku University Graduate School of Medicine, Aoba-ku, Sendai, Japan; and the [2]Division of Molecular Metabolism and Diabetes, Tohoku University Graduate School of Medicine, Aoba-ku, Sendai, Japan.
Corresponding author: Hideki Katagiri, katagiri@med.tohoku.ac.jp.
Received 7 June 2010 and accepted 30 October 2010.
DOI: 10.2337/db10-0796
This article contains Supplementary Data online at http://diabetes.diabetesjournals.org/lookup/suppl/doi:10.2337/db10-0796/-/DC1.
T.S. and J.I. contributed equally to this work.

Animals. Animal studies were conducted in accordance with Tohoku University institutional guidelines. We used 8-week-old C57Bl/6N male mice, purchased from Kyudo (Kumamoto, Japan), for in vivo gene transfer study. Mice were housed in an air-conditioned environment, with a 12-h light-dark cycle (light on at 09:00 A.M.), and fed a regular unrestricted diet.

Glucose, insulin, and pyruvate tolerance tests. Glucose tolerance tests (GTT) were performed on fasted (10 h, daytime) mice. Mice were given glucose (2 g/kg of body wt) intraperitoneally, followed by measurement of blood glucose level (13). Insulin tolerance tests (ITT) were performed on ad libitum-fed mice. Mice were intraperitoneally injected with human regular insulin (0.25 units/kg of body wt; Eli Lilly, Kobe, Japan), followed by measurement of blood glucose level (14). Pyruvate tolerance tests were performed on fasted (10 h, daytime) mice. Mice were intraperitoneally injected with sodium pyruvate (2 g/kg of body wt; SIGMA, St. Louis, MO) dissolved in PBS, followed by measurement of blood glucose levels.

Blood analysis. Blood samples were obtained from fasted (10 h, daytime) mice. Blood glucose was assayed with Antsense-III (Horiba Industry, Kyoto, Japan). ELISA kits were used to measure plasma insulin, leptin (Morinaga, Tokyo, Japan), IL-6 (eBioscience, San Diego, CA), adiponectin (Ohtsuka Pharamaceutical, Tokyo, Japan), tumor necrosis factor-α (TNF-α) (R&D Systems, Minneapolis, MN), and glucagon (Wako Pure Chemical, Osaka, Japan) levels. Plasma free fatty acid (FFA) levels were determined with an NEFA C (Wako Pure Chemical, Osaka, Japan) kit. Plasma transaminase levels were determined with a Transaminase C II-test (Wako Pure Chemical, Osaka, Japan) kit.

Immunoblotting. Liver samples obtained from fasted (10 h, daytime) mice were prepared, and tissue protein extracts (250 μg total protein) were boiled in Laemmli buffer containing 10 mmol/L dithiothreitol, subjected to SDS-polyacrylamide gel electrophoresis (15). Antibody to IL-6 (MAB406, R&D Systems) was commercially obtained.

Pancreatic insulin content. Pancreata were suspended in cold acid ethanol (1.5% HCl in 75% ethanol) and minced with scissors, and left at −20°C for 48 h, with sonication every 24 h (16). Insulin contents in the acid ethanol supernatant were determined with an ELISA kit (Morinaga).

Hepatic triglyceride content. Frozen livers were homogenized, and triglycerides were extracted with $CHCl_3$:CH_3OH (2:1, vol:vol), dried, and resuspended in 2-propanol (14). Triglyceride contents were measured using a Lipidos liquid kit (TOYOBO, Osaka, Japan).

Oxygen consumption. Oxygen consumption was measured with an O_2/CO_2 metabolism measuring system (model MK-5000RQ; Muromachikikai, Tokyo, Japan). Each mouse was kept unrestrained in a sealed chamber with an airflow of 0.5 L/min for 24 h at 25°C. Air was sampled every 3 min, and oxygen consumptions were calculated.

Cell culture. The insulin-secreting β-cell line MIN-6 was maintained in Dulbecco's Modified Eagle Medium containing 25 mM glucose supplemented with 10% fetal calf serum.

Studies with isolated islets and MIN-6 cells. Pancreatic islets were isolated from 8-week-old C57Bl/6N male mice by retrograde injection of collagenase (Sigma) into the pancreatic duct according to the standard procedure as described previously (16). Isolated islets were maintained in RPMI1640 medium containing 11.1 mmol/L glucose. For insulin secretion studies, batches of 10 islets or MIN-6 cells were cultured in the medium under several conditions and then washed with modified Krebs–Ringer bicarbonate buffer (KRBB). After a 30-min preincubation in KRBB containing 1.67 mmol/L glucose, islets or cells were treated for 60 min in KRBB supplemented with either 1.67 or 16.7 mmol/L glucose. Insulin contents of isolated islets or MIN-6 cells were measured after acid ethanol extraction. Recombinant murine IL-6 (PeproTech, London, U.K.), U-73343, U-73122, neomycin (Sigma), Xestospongin C (Biomol, Plymouth Meeting, PA), and H-89 (Millipore, Billerica, MA) were commercially obtained.

Histological analysis. The liver, adipose tissue, and pancreas from LacZ- and IL-6 mice were fixed with 10% formalin, embedded in paraffin, and sectioned. Sections were stained with hematoxylin and eosin. For measurement of β-cell areas, consecutive paraffin sections 500 μm apart spanning the entire pancreas (excised on 14 days after adenoviral treatments) were stained for insulin and with hematoxylin and eosin. After staining, β-cell areas were measured in all sections with Scion Image software (Scion Corporation, Frederick, MD) as described previously (17).

Evaluation of gene expression by RT-PCR. Total RNAs were isolated from 50 mg of hepatic tissue from 10 h-fasted mice on day 5 after adenoviral administration. cDNAs synthesized from 1.0 μg of total RNAs with a First Strand cDNA Synthesis Kit (Roche, Indianapolis, IN) as described previously (18) were evaluated with a real-time PCR quantitative system (Light Cycler Quick System 350S; Roche Diagnostics, Mannheim, Germany), with the oligonucleotides presented in Supplementary Table 1.

The relative amount of mRNA was calculated with β-actin mRNA as the invariant control.

Small interfering RNA transfection. All small interfering RNA (siRNA) oligonucleotides (ON-TARGETplus SMART pool) were purchased from Thermo Fisher Scientific (MA). MIN-6 cells were transfected with siRNAs using DhamaFECT 1 Transfection Reagent (Thermo Fisher Scientific).

Statistical analysis. All data were expressed as means ± SE. For experiments in which data differences needed to be assessed among three or more groups, we used one-way ANOVA followed by Bonferroni's post hoc test. In experiments in which data differences between two groups were assessed, results were analyzed using the unpaired *t* test.

RESULTS

Adenoviral overexpression of IL-6 elevates plasma IL-6 concentrations and reduces adipose tissue. To explore the role of IL-6 in β-cell function, we prepared recombinant adenovirus containing mouse IL-6 cDNA and injected 3×10^7 PFU IL-6 adenovirus intravenously into C57BL/6N mice (IL-6 mice). Mice administered adenovirus containing the *LacZ* gene were used as controls (LacZ-mice). Immunoblotting of hepatic lysates on day 5 after adenoviral administration confirmed overproduction of IL-6 in the livers of IL-6 mice (Fig. 1*A*). As reported previously (12,17,19), systemic infusion of recombinant adenovirus resulted in selective transgene expression in the liver with no detectable expression in other tissues (data not shown). Thus hepatic overexpression of IL-6 was achieved and IL-6 produced in the liver was secreted into the systemic circulation, resulting in significant plasma IL-6 elevation, with concentrations peaking at 1,407 ± 368 pg/mL on day 5 after adenoviral administration (Fig. 1*B*). These plasma IL-6 concentrations in IL-6 mice were within the range of those observed in *ob/ob* and *db/db* mice, murine models of severe obesity (20–22). In contrast, plasma concentrations of TNF-α, another proinflammatory cytokine related to obesity, were similar in these two groups of mice (Fig. 1*C*). Plasma glucagon concentrations were significantly higher in IL-6 mice (Fig. 1*D*) than in control mice, which is consistent with the previous report that IL-6 KO mice exhibited low glucagon levels (3). Body weights tended to be reduced in IL-6 mice as compared with those in LacZ-mice and mice without adenoviral administration, although the differences did not reach statistical significance (Fig. 1*E*). No hepatic architecture changes or cell infiltrations were revealed by histological analyses in IL-6 mice (Fig. 1*F*). Circulating concentrations of transaminases (Fig. 1*G*), liver weights (Fig. 1*H*), and hepatic triglyceride content (Fig. 1*I*) were similar in IL-6 and LacZ-mice.

Consistent with the findings in mice with IL-6 overexpression in muscle (10), IL-6 mice exhibited reductions in fat masses, i.e., epididymal fat weights (Fig. 2*A*) and the size of adipocytes, compared with LacZ-mice (Fig. 2*B*). Daily food intakes of IL-6 mice were decreased (Fig. 2*C*), and resting oxygen consumptions were significantly increased in IL-6 mice (Fig. 2*D*). The resultant negative energy balance may explain fat mass reductions. One-shot intracerebroventriclar administration of IL-6 reportedly increased energy expenditure (23) and decreased food intake (24). Because IL-6 reportedly passes across the blood-brain barrier (25), the chronic hyper-IL-6-emia observed in IL-6 mice might affect the central nervous system. Consistent with the fat mass reduction, circulating leptin concentrations were decreased in IL-6 mice (Fig. 2*E*). However, circulating adiponectin concentrations were decreased in IL-6 mice (Fig. 2*F*). This result may be explained by the reported finding that IL-6 has an inhibitory effect on adiponectin production by adipocytes (10,26,27).

IL-6 mice exhibit enhancement of GSIS. Next, to explore the impact of circulating IL-6 elevation on glucose metabolism, intraperitoneal GTT were performed on day 5

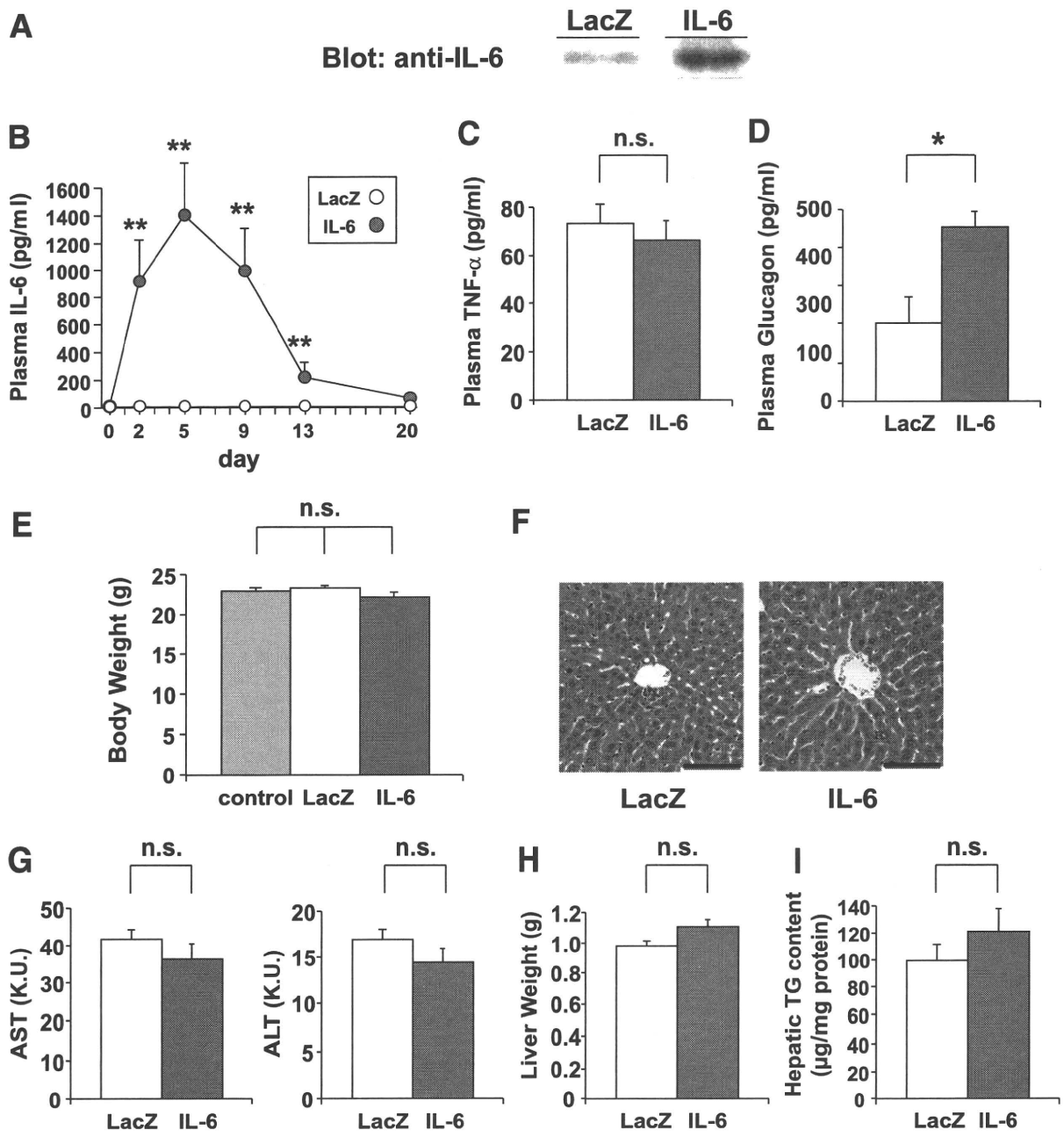

FIG. 1. Adenoviral overexpression of IL-6 raises plasma IL-6 concentrations. Eight-week-old C57Bl/6N male mice were administered adenovirus containing the *LacZ* or the *IL-6* gene. *A*: Immunoblotting of hepatic lysates with anti-IL-6 antibody on day 5 after adenoviral administration. *B*: Plasma IL-6 concentrations were measured in LacZ- (open circles; $n = 5$) and IL-6 (closed circles; $n = 7$) mice through day 20 after adenoviral administration. *C*: Plasma TNF-α concentrations were measured in LacZ- (open bar; $n = 5$) and IL-6 (closed bar; $n = 7$) mice on day 5 after adenoviral administration. *D*: Fasting plasma glucagon levels were measured in LacZ- (open bar; $n = 4$) and IL-6 (closed bar; $n = 4$) mice on day 5 after adenoviral administration. *E*: Body weights of control (not administered adenovirus) (shaded bar; $n = 5$), LacZ- (open bar; $n = 5$), and IL-6 (closed bar; $n = 7$) mice on day 7 after adenoviral administration. *F*: Histological findings of the liver with hematoxylin and eosin staining on day 5 after adenoviral administration. Scale bars indicate 100 μm. *G–I*: Plasma aspartic aminotransferase (AST) and alanine aminotransferase (ALT) levels (*G*), liver weights (*H*), and hepatic triglyceride content (*I*) were measured in LacZ- (open bars; $n = 5$) and IL-6 (closed bars; $n = 7$) mice on day 5 after adenoviral administration. *$P < 0.05$; **$P < 0.01$ vs. LacZ-mice assessed by unpaired *t* test in *B–D*, *G–I*, and by one-way ANOVA followed by Bonferroni's post hoc test in *E*. Data are presented as means ± SE. (A high-quality digital representation of this figure is available in the online issue.)

after adenoviral administration. IL-6 mice exhibited marked improvement of glucose tolerance compared with LacZ-mice (Fig. 3*A*). Plasma insulin and C-peptide concentrations after glucose loading were remarkably higher in IL-6 mice than in LacZ-mice, whereas fasting insulin and C-peptide levels were similar in these two groups (Fig. 3*B* and *C*). In contrast, ITT revealed no significant difference in insulin sensitivity between these two groups of mice (Fig. 3*D*). These findings indicate that improvement of glucose tolerance, especially after glucose loading, in IL-6 mice is attributable to enhancement of GSIS. On the other hand, pancreatic islet sizes were apparently similar in LacZ- and IL-6 mice (Fig. 3*E*). Quantitatively, β-cell areas (Fig. 3*F*) and pancreatic insulin content (Fig. 3*G*) did not differ between these groups of mice.

Fasting blood glucose levels were also lowered in IL-6 mice, and this effect persisted for 14 days after adenoviral administration (Fig. 3*H*). This result is compatible with the

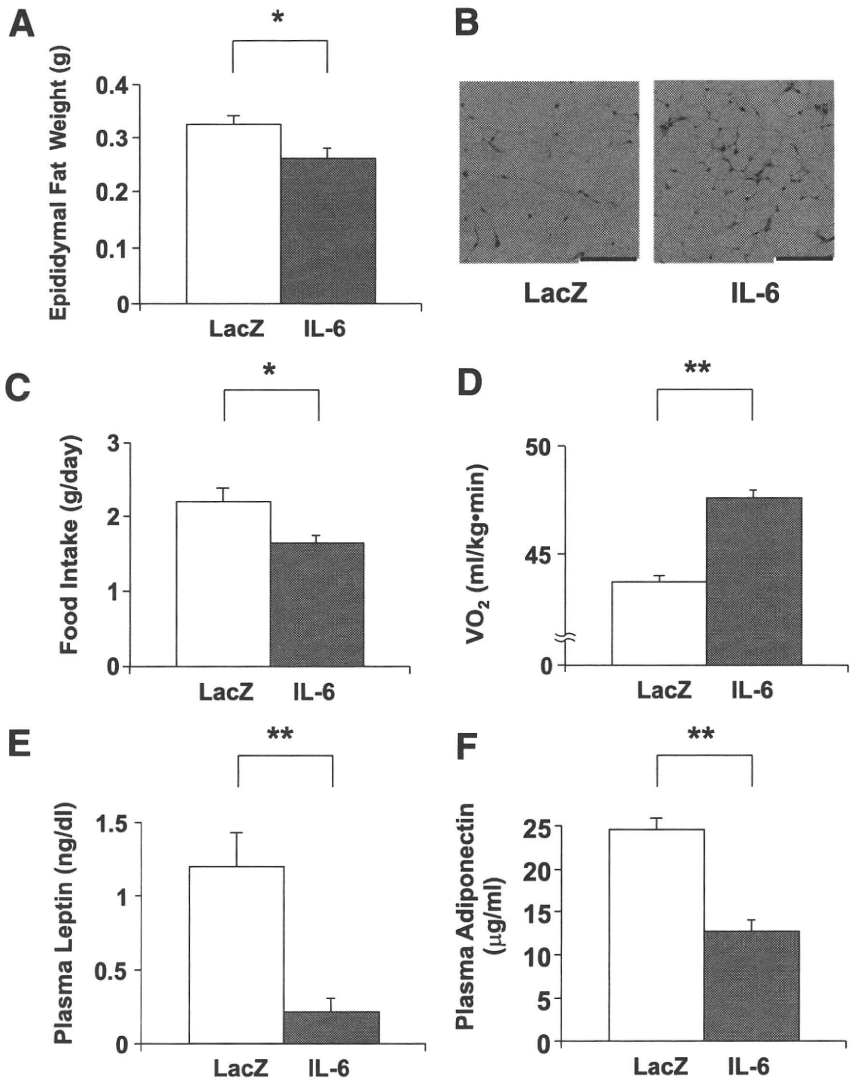

FIG. 2. Adenoviral overexpression of IL-6 reduces adipose tissue. *A*: Epididymal fat weights in LacZ- (open bar; $n = 5$) and IL-6 (closed bar; $n = 7$) mice were measured on day 5 after adenoviral administration. *B*: Histological findings of the epididymal fat tissue with hematoxylin and eosin staining on day 5 after adenoviral administration. Scale bars indicate 100 μm. *C*: Mean daily food intakes for 5 days were calculated in LacZ- (open bar; $n = 5$) and IL-6 (closed bar; $n = 7$) mice. *D–F*: Resting oxygen consumption ($n = 3$ per group) (*D*) and plasma levels of leptin (*E*) and adiponectin (*F*) were measured in LacZ- (open bars; $n = 5$) and IL-6 (closed bars; $n = 7$) mice. *$P < 0.05$; **$P < 0.01$ vs. LacZ-mice assessed by unpaired *t* test. Data are presented as means ± SE. (A high-quality digital representation of this figure is available in the online issue.)

exogenous expression period for adenoviral gene transduction (19). IL-6 reportedly activates the signal transducer and activator of transcription-3 (STAT-3) signaling, leading to downregulation of gluconeogenic genes in hepatocytes (28). Consistent with this notion, expressions of gluconeogenic genes, such as phosphoenolpyruvate carboxykinase and glucose-6-phosphatase, were significantly decreased in the livers of IL-6 mice (Fig. 3*I*). In addition, pyruvate tolerance tests revealed that blood glucose levels after pyruvate loading were significantly lower in IL-6 mice than in LacZ-mice (Fig. 3*J*). These findings together indicate that hepatic glucose production was suppressed in IL-6 mice, supporting the previously reported observation that hepatic gluconeogenic gene expressions and fasting blood glucose levels were suppressed in mice with muscle-specific IL-6 overexpression (10).

A lipolytic effect of IL-6 was previously reported (29), and lipolysis raises circulating FFA concentrations. Because FFAs are known to be potent insulinotropic factors (30), we evaluated plasma FFA concentrations. However, plasma FFA concentrations of IL-6 mice on day 5 after adenoviral administration did not differ significantly from those of LacZ-mice (Fig. 3*K*). Thus FFAs are unlikely to be involved in the enhancement of GSIS in IL-6 mice.

IL-6 enhances GSIS from both isolated pancreatic islets and MIN-6 cells. These in vivo findings prompted us to investigate the direct effects of IL-6 on pancreatic β-cells. Therefore, we isolated pancreatic islets from C57BL/6N mice, and the isolated islets were incubated in medium containing 1,200 pg/mL recombinant IL-6 for 48 h, followed by examination of GSIS. Note that the IL-6 concentrations used in these in vitro experiments were similar to the plasma IL-6 concentrations in IL-6 mice on day 5 after adenoviral administration (Fig. 1*B*). At this time point, GSIS enhancements were observed in IL-6 mice (Fig. 3*B*). As shown in Fig. 4*A*, IL-6 pretreatment markedly enhanced insulin secretion in response to 16.7 mmol/L glucose, whereas enhancement of insulin secretion was not statistically significant at 1.67 mmol/L glucose. Pretreatment with IL-6 at a lower concentration, 600 pg/mL,

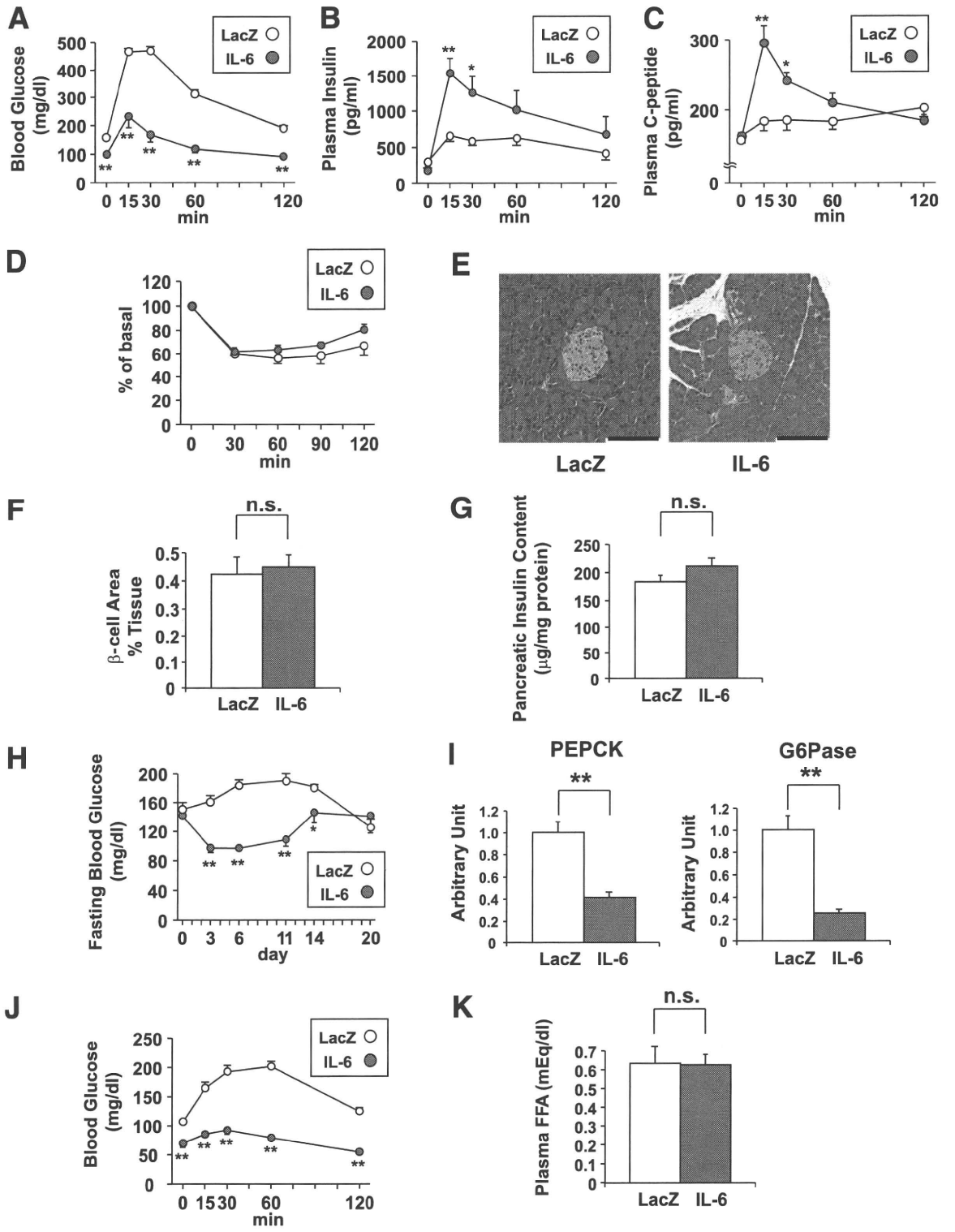

FIG. 3. Adenoviral overexpression of IL-6 enhances GSIS. *A–C*: Blood glucose (*A*), plasma insulin (*B*), and plasma C-peptide (*C*) levels during glucose tolerance tests performed in LacZ- (open circles; $n = 5$) and IL-6 (closed circles; $n = 7$) mice on day 5 after adenoviral administration. Statistical significance was calculated using the unpaired t test. *D*: Blood glucose levels after intraperitoneal insulin injection in LacZ- (open circles; $n = 5$) and IL-6 (closed circles; $n = 7$) mice on day 7 after adenoviral administration. Data are presented as percentages of the blood glucose levels immediately before insulin loading. *E*: Histological findings of the pancreas with hematoxylin and eosin staining on day 5 after adenoviral administration. Scale bars indicate 100 μm. *F*: β-cell areas of LacZ- (open bars; $n = 5$) and IL-6 (closed bars; $n = 7$) mice on day 14 after adenoviral administration. *G*: Pancreatic insulin contents were determined in LacZ- (open bars; $n = 5$) and IL-6 (closed bars; $n = 7$) mice on day 14 after adenoviral administration. *H*: Fasting blood glucose levels were measured in LacZ- (open circles; $n = 5$) and IL-6 (closed circles; $n = 7$) mice through day 20 after adenoviral administration. *I*: Hepatic expressions of PEPCK (*left*) and glucose-6 (*right*) of LacZ- (open bars; $n = 5$) and IL-6 (closed bars; $n = 7$) mice were analyzed by RT-PCR. *J*: Blood glucose levels during pyruvate tolerance tests performed in LacZ- (open circles; $n = 5$) and IL-6 (closed circles; $n = 7$) mice on day 5 after adenoviral administration. *K*: Fasting plasma free fatty acid levels were measured in LacZ- (open bar; $n = 5$) and IL-6 (closed bar; $n = 7$) mice on day 5 after adenoviral administration. $^*P < 0.05$; $^{**}P < 0.01$ vs. LacZ-mice assessed by unpaired t test. Data are presented as means ± SE. (A high-quality digital representation of this figure is available in the online issue.)

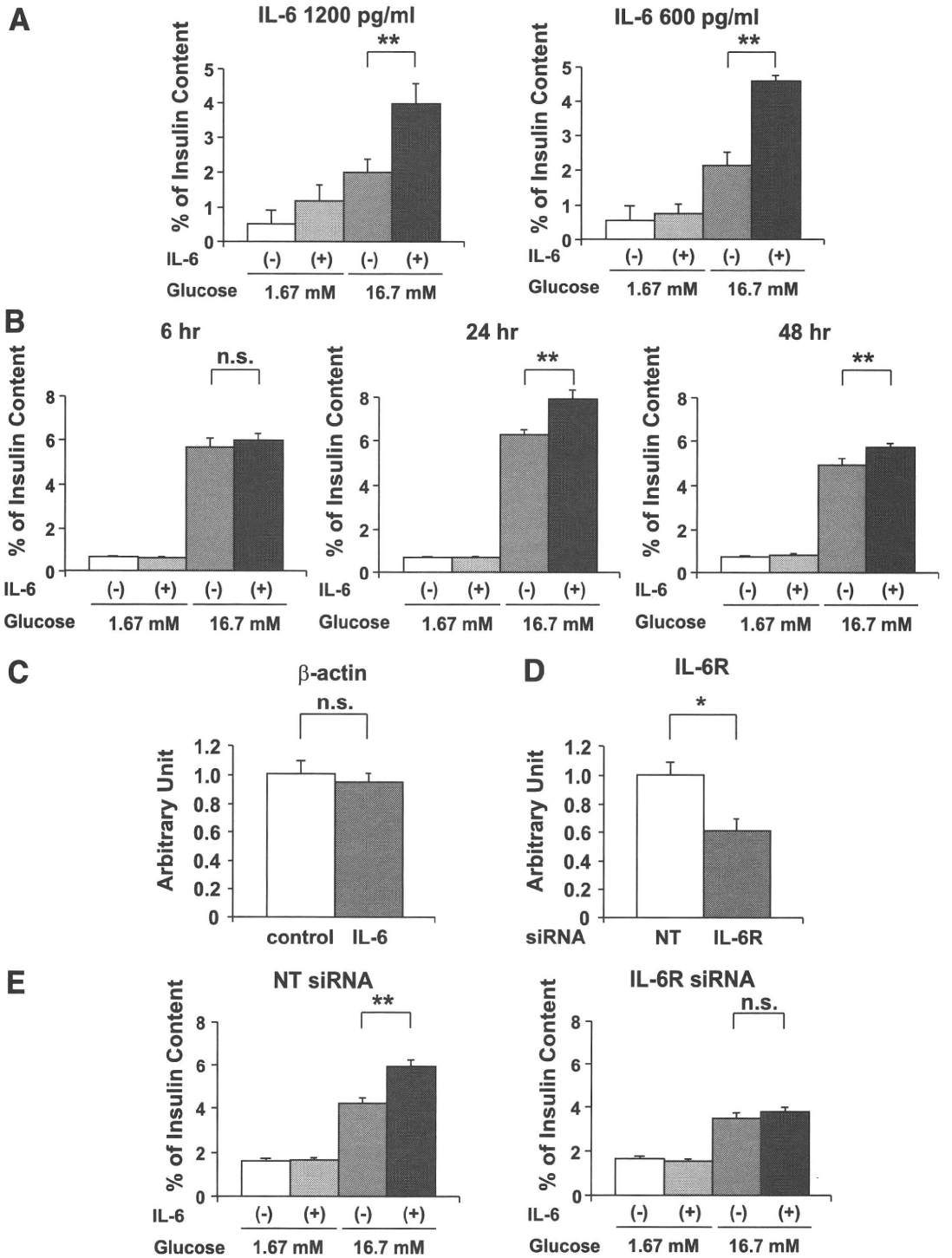

FIG. 4. IL-6 enhances GSIS from both isolated pancreatic islets and MIN-6 cells. *A*: Pancreatic islets were isolated from 8-week-old C57BL/6N mice and then incubated with or without 1,200 or 600 pg/mL recombinant IL-6 for 48 h, followed by examination of insulin secretion for 60 min in KRBB supplemented with either 1.67 or 16.7 mmol/L glucose (n = 4 per group). **P < 0.01 vs. insulin secretion from islets without IL-6 pretreatment assessed by one-way ANOVA followed by Bonferroni's post hoc test. *B*: MIN-6 cells were incubated with or without 1,200 pg/mL recombinant IL-6 for the indicated periods, followed by measurement of insulin secretion for 60 min in KRBB supplemented with either 1.67 or 16.7 mmol/L glucose (n = 6 per group). **P < 0.01 vs. insulin secretion from MIN-6 cells without IL-6 pretreatment assessed by one-way ANOVA followed by Bonferroni's post hoc test. *C*: MIN-6 cells were incubated with or without 1,200 pg/mL recombinant IL-6 for 24 h; the cells were used for RT-PCR analysis. β-actin expression levels of MIN-6 cells were quantified and normalized relative to glyceraldehyde-3-phosphate dehydrogenase (GAPDH) mRNA levels. Difference was assessed by unpaired t test. *D*: Nontargeting (NT) siRNA (open bars; n = 5) or IL-6R siRNA (closed bar; n = 5) were applied to the MIN-6 cells. After 48 h incubation, the cells were used for RT-PCR analysis. IL-6R expression levels of MIN-6 cells were quantified and normalized relative to β-actin mRNA levels. *P < 0.05 vs. NT siRNA transfected MIN-6 cells assessed by unpaired t test. *E*: Knockdown of IL-6R inhibited IL-6-mediated enhancement of GSIS from MIN-6 cells. MIN-6 cells were transfected with NT siRNA or IL-6R siRNA for 24 h and then incubated with or without concomitant 1,200 pg/mL recombinant IL-6 for 24 h, followed by examination of insulin secretion for 60 min in KRBB supplemented with either 1.67 or 16.7 mmol/L glucose (n = 5 per group). **P < 0.01 vs. insulin secretion from MIN-6 cells without IL-6 pretreatment assessed by one-way ANOVA followed by Bonferroni's post hoc test. Data are presented as means ± SE.

also significantly enhanced GSIS from isolated islets (Fig. 4*A*), although insulin content in isolated islets was not altered by IL-6 pretreatment (Supplementary Table 2). Thus IL-6 directly enhances insulin secretion, particularly in response to a high concentration of glucose.

We further confirmed the direct effect of IL-6 on GSIS using MIN-6 cells, a murine β-cell line that is widely accepted as maintaining glucose responsiveness of insulin secretion in a fashion similar to that in primary pancreatic β-cells (31). MIN-6 cells were incubated in medium containing 1,200 pg/mL recombinant IL-6 for several periods, followed by examinations of GSIS. Although no enhancement of insulin secretion was observed after 6-h incubation with IL-6, significant increments in glucose (16.7 mmol/L)-induced insulin secretion were observed in MIN-6 cells pretreated with IL-6 for more than 24 h, as compared with IL-6-untreated MIN-6 cells. However, no enhancement of insulin secretion was observed at low glucose (1.67 mmol/L) even after 24 h stimulation with IL-6 (Fig. 4*B*). Thus these data clearly showed that IL-6 directly enhances GSIS from pancreatic β-cells. Because a 24-h IL-6-pretreatment period exerted the GSIS-enhancing maximal effect, we performed the following experiments using MIN-6 cells pretreated for 24 h with IL-6 (Fig. 4*B*). Under these conditions, neither insulin content (Supplementary Table 2) nor β-actin expression (Fig. 4*C*) was significantly altered in MIN-6 cells.

Next, to examine whether the effect of IL-6 on enhanced GSIS from MIN-6 cells is actually mediated by the IL-6R, we knocked down IL-6R expression using a specific siRNA. The specific siRNA for the IL-6R significantly reduced expression of IL-6R mRNA in MIN-6 cells (Fig. 4*D*). Suppression of IL-6R expression markedly blunted IL-6-mediated enhancement of GSIS from MIN-6 cells. These findings indicate that the IL-6R is substantially and functionally expressed in MIN-6 cells and that IL-6 exerts its stimulatory effects on GSIS through the IL-6R (Fig. 4*E*).

IL-6–induced enhancement of GSIS is abrogated by PLC pathway inhibitors. Acetylcholine has been shown to enhance GSIS from β-cells, and this GSIS enhancement is mediated, at least partially, by the PLC pathway (32). In addition, IL-6 reportedly activates the PLC pathway in a few other cell types (33,34). Therefore, we next examined involvement of the PLC pathway in IL-6–induced enhancement of GSIS. Isolated pancreatic islets and MIN-6 cells were pretreated with 2 μmol/L U-73122, a PLC inhibitor (35), with or without concomitant 1,200 pg/mL IL-6 for 24 h, followed by measurement of GSIS. As shown in Fig. 5*A* and *B*, IL-6–induced enhancement of GSIS from both isolated pancreatic islets and MIN-6 cells was almost completely abolished with U-73122. We then further confirmed involvement of the PLC pathway in IL-6–induced enhancement of GSIS from MIN-6 cells, using another PLC inhibitor, neomycin. This compound inhibits PLC activity by binding to phosphatidylinositol 4,5-bisphosphatase (PIP_2) (35). Again, pretreatment with 1.5 mmol/L neomycin inhibited IL-6–induced enhancement of GSIS from MIN-6 cells (Fig. 5*C*). Thus two PLC inhibitors, with different mechanisms of action, inhibited IL-6–induced enhancement of GSIS, strongly suggesting that the underlying mechanism is mediated by the PLC pathway.

PLC-β1 is involved in IL-6–induced enhancement of GSIS. To examine which isoform(s) of PLC is involved in IL-6–induced enhancement of GSIS, we knocked down several isoforms of PLC in MIN-6 cells, followed by testing IL-6–induced GSIS. We selected PLC isoforms reportedly expressed in pancreatic islets or a β-cell line (32,36,37) and prepared specific siRNAs for each isoform. Specific siRNAs for PLC-β1, -β_2, -β_3, -γ_1, -γ_2, and -δ_1 significantly suppressed the expression of each PLC isoform in MIN-6 cells (Supplementary Fig. 1). In addition, knockdown of PLC-β_1 and PLC-γ_1 was confirmed by immunoblotting (Supplementary Fig. 2). Among them, in PLC-β_1-knockdown MIN-6 cells, IL-6 pretreatment did not enhance GSIS (Fig. 5*D*). These results suggest that PLC-β_1 is involved in the stimulatory effects of IL-6 on GSIS.

IL-6–induced enhancement of GSIS is not abrogated by a PKA inhibitor. The cyclic AMP (cAMP)-protein kinase A (PKA) pathway, activated by incretins or glucagon, is also well known to enhance GSIS from pancreatic β-cells. Therefore, we next examined the possible involvement of the PKA pathway in IL-6–induced enhancement of GSIS from MIN-6 cells. MIN-6 cells were pretreated with 1 μmol/L H-89, a selective PKA inhibitor (38), with or without concomitant 1,200 pg/mL IL-6 for 24 h, followed by measurement of GSIS. In contrast with the PLC pathway inhibitors, H-89 did not inhibit IL-6–induced enhancement of GSIS from MIN-6 cells (Fig. 6*A*), suggesting a contribution of the cAMP-PKA pathway to IL-6–induced enhancement of GSIS to be unlikely.

IL-6–induced enhancement of GSIS is abrogated by an IP_3 receptor antagonist. The aforementioned results suggest that the PLC pathway is involved in IL-6-mediated enhancement of GSIS. We further examined the downstream pathway from PLC through GSIS enhancement. PLC activation reportedly leads to hydrolysis of PIP_2 into diacylglycerol and IP_3. IP_3 binds to the IP_3 receptor on the endoplasmic reticulum (ER), resulting in the induction of Ca^{2+} release from the ER. This leads to an elevation of the cytoplasmic free Ca^{2+} concentration and subsequently increases insulin secretion (39). To examine whether this mechanism is involved, MIN-6 cells were pretreated with 10 μmol/L Xestospongin C, an IP_3 receptor antagonist (40), with or without concomitant 1,200 pg/mL IL-6 for 24 h, followed by examination of GSIS. Xestospongin C pretreatment decreased insulin content of MIN-6 cells, unlike pretreatments with IL-6, inhibitors, or siRNAs described above (Supplementary Table 2) but did not affect insulin secretion at low (1.67 mM) and high (16.7 mM) concentrations of glucose, when expressed as percentage of insulin content (Fig. 6*B*). In addition, IL-6 pretreatments did not alter insulin content of Xestospongin C-treated MIN-6 cells (Supplementary Table 2). Under these conditions, Xestospongin C inhibited IL-6–induced enhancement of GSIS from MIN-6 cells (Fig. 6*B*). Collectively, these findings indicate that IL-6 directly enhances insulin secretion in response to glucose stimulation through the PLC-IP_3–dependent pathway.

DISCUSSION

IL-6 exerts its effects through binding to a receptor complex consisting of two transmembrane glycoproteins, the specific receptor subunit IL-6R and a 130-kDa signal transducing protein (gp130). Formation of the hexametric IL-6/IL-6R/gp130 complex initiates activation of two major signaling pathways, Janus kinase (JAK)-STAT and the mitogen-activated protein kinase (1). Recently, expressions of both IL-6R and gp130 in murine β-cells were reported, and notably, the expression levels of these molecules were comparable with those in muscle (3), suggesting substantial impacts of IL-6 on pancreatic β-cells. However,